e-ISSN:2602-2079

Volume 9
Issue 7
2025

JOURNAL of Surgery and Medicine

International Medical Journal

JOSAM

Editorial Team

Kuwait City, Hawally, Kuwait
Website
Email

Fahmi Khan, MB, BS, CABMs
Hamad Medical Corporation | HMC
Department of Medicine (Hamad General Hospital)
Doha, Qatar
Website
Email

Elroy Patrick Weledji, Professor, BSc, MBBChBAO, MSc, FRCS(Edinburgh)
Department of Medicine
University of Buea
Buea, Cameroon
Website
Email

Prasenjit Das, Professor, MD, DNB, MNAMS, MNASc
Department of Pathology
All India Institute of Medical Sciences
New Delhi, India
Website
Email

Seyed Vahid Hosseini, Professor
Shiraz University of Medical Sciences, Shiraz, Iran
Website
Email

Vol. 9 No. 7 (2025)

Published: 2025-07-25

Research Article

Case Report

J Surg Med. 2025;9(7):93-97.
https://doi.org/10.28982/josam.8060

JOSAM

Research article
https://jsurgmed.com/

Journal of Surgery and Medicine

e-ISSN: 2602-2079

The relationship of PAPP-A and ß-HCG values with fetal gender and fetal birth weight: A single-center experience

Şükriye Leyla Altuntaş [1], Adeviye Elçi Atılgan [2], Fatma Kılıç [3]

[1] Department of Obstetrics and Gynecology, Istanbul Medipol University Faculty of Medicine, İstanbul, Turkey
[2] Department of Obstetrics and Gynecology, Umut Hospital, Ordu, Turkey
[3] Department of Obstetrics and Gynecology, Necmettin Erbakan University Meram Faculty of Medicine, Konya, Turkey

ORCID of the author(s)

ŞLA: https://orcid.org/0000-0003-1985-552X
AEA: https://orcid.org/0000-0003-4833-8978
FK: https://orcid.org/0000-0002-9735-3552

Corresponding Author
Adeviye Elçi Atılgan
Department of Obstetrics and Gynecology, Umut Hospital, Ordu, Turkey
E-mail: dradeviye@gmail.com

Ethics Committee Approval
The study was approved by the Educational Planning Coordination Board of Istanbul Medipol University Hospital (E -10840098-772.02-780 / January 30, 2023).
All procedures in this study involving human participants were performed in accordance with the 1964 Helsinki Declaration and its later amendments.

Conflict of Interest
No conflict of interest was declared by the authors.

Financial Disclosure
The authors declared that this study has received no financial support.

Published
2025 July 4

Abstract

Background/Aim: Intrauterine growth restriction (IUGR) is a multisystem disorder that results in perinatal morbidity and mortality due to decreased oxygen transfer from mother to fetus, a consequence of placental dysfunction. The placenta secretes certain unique proteins, the levels of which significantly rise in maternal blood during pregnancy. Among these, free beta-human chorionic gonadotropin (ß-HCG) and Pregnancy-Associated Plasma Protein-A (PAPP-A) are the most frequently analyzed. Our primary aim was to assess the correlation between PAPP-A and free ß-HCG levels, derived from the first-trimester dual-screening test, with fetal sex and birth weight. Our secondary aim was to determine the possibility of predicting IUGR using these markers.
Methods: The first-trimester screening data, along with fetal sex and birth weight, of singleton pregnancies in either primiparous or multiparous women who attended Istanbul Koşuyolu Medipol Hospital and gave birth during the first trimester, were retrospectively analyzed from the hospital file system.
Results: PAPP-A demonstrated a positive correlation with birth weight. It was significantly lower in cases of IUGR compared to normal fetal birth weight. A statistically significant correlation was also found between fetal gender and both ß-HCG and PAPP-A values; they were both higher in girls compared to boys ($P<0.05$).
Conclusions: Pregnancies with low PAPP-A values in first-trimester screenings should be closely monitored for IUGR. As PAPP-A and ß-HCG averages were found to be lower in boys, they appear more risky. At this point, a larger number of multicentric prospective studies are needed to support this conclusion.

Keywords: adverse pregnancy outcomes, pregnancy-associated plasma protein-A, ß-HCG, dual test

How to cite: Altuntaş ŞL, Elçi Atılgan A, Kılıç F. The relationship of PAPP-A and ß-HCG values with fetal gender and fetal birth weight: A single-center experience. J Surg Med. 2025;9(7):93-97.

Introduction

Today, early detection of Intrauterine Growth Restriction (IUGR) is critical during prenatal check-ups to avoid multi-organ failure. It is understood that the fundamental pathophysiological cause of IUGR is placental dysfunction. This dysfunction occurs via excessive vasoconstriction of the uterine and placental spiral arteries, leading to reduced oxygen delivery to the fetus and, thus, limited intrauterine fetal growth [1].

During pregnancy, the placenta secretes unique proteins, and their levels in the maternal blood increase measurably. Among these, free beta-human chorionic gonadotropin (ß-HCG) and Pregnancy-Associated Plasma Protein-A (PAPP-A) are the most commonly used markers in studies [1]. ß-HCG and PAPP-A are measured in pregnant plasma and, combined with maternal age and Nuchal translucency (NT), are used as screening tests to identify the likelihood of various aneuploidies, particularly Down syndrome [2,3]. The first-trimester screening test, also known as the double test, is performed during the 11th to 14th gestational weeks. It provides insights into potential fetal anomalies and enables the termination of pregnancy in earlier weeks. A variety of studies have examined the relationship between fetal weight and PAPP-A [3-5]. However, there has been no study exploring the relationship between the values from the double-screening test and both fetal gender and weight.

In this study, we aimed to explore whether there is any association between maternal PAPP-A and ß-HCG levels, obtained from the dual-screening test in the first trimester of pregnancy, and fetal sex as well as fetal birth weight. We also investigated the possibility of predicting IUGR using these markers.

Materials and methods

This retrospective study was conducted at Koşuyolu Medipol University Hospital from January 1, 2009, to December 31, 2016. The subjects included primiparous and multiparous singleton pregnancies who underwent dual-screening tests and follow-up visits at our hospital and also delivered their babies here. A total of 1022 primiparous or multiparous pregnant women who had such screening tests in our biochemistry laboratory were selected for examination. Informed consent was obtained from all participants. Ethical approval was granted by the Educational Planning Coordination Board of Istanbul Medipol University Hospital (E-10840098-772.02-780).

All data was analyzed retrospectively from hospital file records. Not included were multiple pregnancies, pregnant women who smoked, those who miscarried or gave birth prematurely, or had their double test at a different center.

Participants were evaluated by a proficient perinatologist with an ultrasound between 11 weeks 4 days to 13 weeks 6 days of pregnancy. First, it was confirmed as a singleton pregnancy by ultrasonography, and the crown-rump length (CRL) and the NT of the fetus were measured. The obtained values were recorded on our hospital's double-screening test printed form, and venous blood samples from the pregnant participants were taken on the same day.

After ultracentrifugation, PAPP-A and free ß-HCG were measured from hemolyzed and non-lipidemic serum samples. Serum biochemical markers were gauged using kits from IMMULITE 2000 and the "solid-phase, enzyme-labeled chemiluminescent immunometric assay" technique, which utilizes the chemiluminescence method. The kit's sensitivity is 0.025 mIU/mL for PAPP-A and 1 ng/mL for free ß-HCG.

The results obtained were tallied with MoM (Multiples of Median) values corrected for case demographic data, maternal age, weight, diabetes, and gestational age. Then, using PRISCA 4.0 (Prenatal risk calculation software from TYPOLOG Software/GmBH, Hamburg, Germany), risks for Biochemical Trisomy 21, age, and a combined risk, which included NT and biochemical parameters, were calculated.

Based on these results, the value of 1/250 was taken as the cut-off value in the first-trimester screening, and patients were counseled whether they were in the high-risk group. At birth, the newborn's Apgar score, gender, fetal length, birth weight, head circumference percentiles, and any congenital deformities and complications at the time of delivery were recorded in the electronic file system.

Statistical analysis

All statistical analyses were conducted using IBM SPSS version 25.0 (SPSS Inc., Chicago, Illinois, USA). The normal distribution of the values was evaluated using the Kolmogorov-Smirnov test with Lilliefors correction. In the tables, continuous variables are presented as mean (standard deviation [SD]), while categorical variables are represented as number (n) and percentage (%). Comparisons between groups were made using the independent t-test for continuous variables. The relationships between continuous variables were analyzed using Pearson correlation. $P<0.05$ was considered statistically significant.

Results

The demographic and clinical characteristics of patients are illustrated in Table 1. The mean age of 1022 singleton pregnant women at birth was 30 (range 17–36) years. The average gestational age at the time of the dual-screening test was 12+4 (11+4–13+6) weeks, or when calculated in days 87.99(3.50) days as shown in Table 2. The median CRL and NT for the fetuses were 60.58 (6.94) mm and 1.67 (0.40) mm respectively. The mean PAPP-A value was 1.01 (0.50) MoM and the mean ß-HCG value was 1.14 (0.73) MoM. The mean gravida was 1.66 (0.80), and the mean body mass index of the patients was 25.20 (11.0) kg/m^2. It was found that 48% (n=490) of the babies born were girls and 51% (n=524) were boys. 19.3% (n=197) of the pregnant women had a normal vaginal delivery, and 80.7% (n=824) had a cesarean section. The mean fetal weight was 3.29 (0.46) kg and the average gestational age at birth was 38.52 (1.54) weeks. A diagnosis of IUGR was given to 10% (n=100) of the pregnant women. As shown in Table 2, there is a significant positive correlation between fetal weight and PAPP-A values (r=0.110, P=0.001). However, no significant relationship was found between fetal weight and ß-HCG values (r=0.016, P=0.303) or NT values and fetal weight (r=0.004, P=0.201). Notably, a negative association was observed between trisomy 21 biochemical risk and fetal weight (r=0.071 P=0.023). Examining the relationship between gender and dual screening test parameters reveals a significant difference between gender and PAPP-A values: a comparative analysis found higher PAPP-A levels in females than in males

(*P*=0.004) (Table 3). Similarly, there is a statistically significant difference between gender and ß-HCG averages: ß-HCG averages were found to be higher in girls than in boys (*P*<0.001) (Table 3).

Table 1: Demographic and clinical features of the subjects included in the study.

Fetal Gender	**n (%) or Mean (SD)**
Female	490 (48.3)
Male	524 (51.7)
Type of delivery	
Vaginal delivery	197 (19.3)
Cesarean Section	824 (80.7)
IUGR	
None	899 (90.0)
Present	100 (10.0)
Macrosomia	
None	903 (90.2)
Present	98 (9.8)
Maternal Age (n=1021)	30.55 (4.35)
Gravidity (n=1014)	1.66 (0.80)
Maternal BMI. kg/m²	25.20 (11.03)
Gestational age *(day) (n=1021)	87.99 (3.50)
CRL mm (n=1020)	60.58 (6.94)
NT mm (n=1021)	1.67 (0.40)
PAPP-A, MoM	1.01 (0.50)
ß-HCG, MoM	1.14 (0.73)
Fetal weight, kg (n=1011)	3.29 (0.46)
Gestational age(week) (n=1007)**	38.52 (1.54)

* Gestational Age at Dual screening time, **Gestational Age at birth

Table 2: Correlation analyses between fetal weight, PAPP-A, ß-HCG, NT, maternal weight, and Trisomy 21 values.

		Fetal weight	**PAPP-A**	**ß-HCG**	**NT**	**Maternal BMI**	**Trisomy 21 risky**
Fetal weight	r	1					
PAPP-A	r	0.110**	1				
	P	**<0.001**					
ß-HCG	r	0.016	0.267**	1			
	P	0.603	**<0.001**				
NT	r	-0.004	-0.048	-0.023	1		
	P	0.901	0.128	0.457			
Maternal BMI	r	0.161**	-0.084**	0.031	0.048	1	
	P	**<0.001**	**0.007**	0.327	0.126		
Trisomy 21 risky	r	-0.071*	-0.518**	0.408**	0.080*	0.127**	1
	P	**0.023**	**<0.001**	**<0.001**	**0.011**	**<0.001**	

** Correlation is significant at the 0.05 level (Pearson correlation test), *** Correlation is significant at the 0.01 level (Pearson correlation test)

Table 3: Comparison of PAPP-A and ß-HCG values with fetal gender.

	Female n=490	**Male n=524**	***P*-value**
PAPP-A, MoM	1.06 (0.53)	0.97 (0.48)	0.004
ß-HCG, MoM	1.25 (0.82)	1.04 (0.62)	<0.001

P-value: independent t-test, values: mean (SD)

Discussion

The primary goal of antenatal biochemical screening tests is to minimize maternal and fetal morbidity and mortality [4-6]. Consequently, the number of studies on these placenta-secreted proteins is increasing significantly. PAPP-A, one of these proteins, was first isolated in a laboratory in 1974 [7]. It is secreted from cytotrophoblasts and can be detected in maternal blood starting the 8th week of gestation [4]. In 1999, PAPP-A, an insulin-like growth factor (IGF), was isolated from a human fibroblast culture medium. PAPP-A has been linked to numerous pathophysiological events associated with IGF-1 and 2 [8]. The IGFs are known to play a significant role in trophoblast invasion into the decidua during pregnancy [9]. Any defects in this pathway could potentially affect fetal growth adversely, due to inadequate placental perfusion, and could be the initial mechanism for various pregnancy complications [9,10]. As pregnancy progresses, levels of PAPP-A in maternal blood increase, rapidly decreasing after birth [7]. A decrease in PAPP-A as compared to a typical pregnancy suggests a riskier pregnancy in terms of chromosomal anomalies and negative pregnancy outcomes [11].

In addition to its role in placental and fetal development in pregnant women, PAPP-A plays a significant part in many physiological and pathological processes in non-pregnant individuals. These include bone development and restructuring, wound healing, atherosclerotic plaque formation in the vascular wall, and hyperplasia in smooth muscle cells in the airways of asthma patients [9,12]. Accurate determination of gestational age is indispensable to the health of both mother and infant, and it is crucial to provide comprehensive counseling on safe and effective methods for terminating pregnancy. While the last menstrual period and the first-trimester ultrasound are frequently used to ascertain gestational age, they have inherent limitations in terms of accuracy and usability. Studies on PAPP-A for determining gestational age are ongoing [13]. In pregnancies marked by Down syndrome, maternal serum PAPP-A levels significantly decrease in the first trimester [14]. Moreover, low PAPP-A levels are detected not only in trisomy 21 but also in other fetal aneuploidies [15]. Additionally, low first-trimester PAPP-A levels are closely associated with in-utero fetal death and low birth weight [14]. Consequently, low first-trimester PAPP-A levels have started to be used to monitor pregnancies for adverse fetal outcomes [15]. Parry et al. [16] found a significant correlation between maternal serum PAPP-A levels and detrimental pregnancy outcomes in nulliparous women. However, the tests' analytical properties do not substantiate their usage as clinical biomarkers predicting adverse pregnancy outcomes, either individually or in combination with maternal clinical characteristics [16].

Kantomaa et al. [17] examined data from a large cohort of pregnant women to assess the relationship between PAPP-A and small for gestational age (SGA). They concluded that a cut-off of 0.4 MoM should be used to gauge the increased risk of SGA [17]. Similarly, Sovio et al. [18] highlighted that lower PAPP-A values were linked with fetal growth restriction. The scenario differs slightly for pregnancies complicated by diabetes: the first-trimester serum screening markers for fetal Down syndrome, PAPP-A, and free ß-HCG, cannot serve as a risk determination tool for obstetric complications like IUGR, macrosomia, and preterm birth [19]. Another crucial point is the assessment of pregnant women who smoke. They were not included in this study due to studies showing that smoker's PAPP-A levels are approximately 15 percent lower than non-smokers [20]. Simulation studies also indicated that the detection of trisomy 21 in smokers using free beta hCG, PAPP-A, and maternal age will decrease by about 5 to 6 percent compared to the general population [20]. A few researchers have also studied the connection between first-trimester maternal PAPP-A levels and adverse obstetric outcomes in cases of isolated preterm oligohydramnios. They concluded that PAPP-A should not be used as a marker in such instances [21].

The present study revealed a statistically significant difference between the mean PAPP-A levels and fetal gender: PAPP-A averages were found to be higher in girls compared to boys. Similarly, we found a statistically significant difference between fetal gender and ß-HCG averages: ß-HCG averages were higher in girls than in boys. In contrast, Çökmez et al. [22] stated that PAPP-A and free β-hCG values were not influenced by the fetal gender. In two studies conducted by Nicolaides in 2000 and 2009, the connection between PAPP-A, ß-HCG, and gender was

discussed. Initially, Cowans et al. [23] examined 2923 normal and 203 Trisomy 21(Tri 21) pregnant women, followed by Spencer et al. [24] who examined 56024 normal and 722 Tri 21 pregnant women in 2009. In both studies, maternal ß-HCG and PAPP-A levels were higher in both normal female fetuses and in female fetuses affected by Tri 21. Since this finding reduced the detection rate of Tri 21 in girls by 1-2%, a gender-based correction was deemed necessary.

Stark et al. [25] demonstrated that maternal physiology varies with fetal sex. Pregnant women carrying a male fetus showed increased vasodilation in response to corticotropin-releasing hormone, as well as greater baseline perfusion than those carrying a female fetus. Preeclamptic women pregnant with a male fetus exhibited significantly reduced vasodilation compared to normotensive women carrying a male fetus. However, microvascular function did not show any significant differences between preeclamptic and normotensive women carrying a female fetus [25].

Broere-Brown et al. [26] discovered that the pulsatility index of the uterine artery in women carrying a male fetus was higher compared to those carrying a female fetus. In addition, women carrying a male fetus were observed notching more often in the Doppler resistance pattern. Reinforcing these findings, Inkster et al. [27] reported that epidemiological studies have identified sex differences linked to various obstetric complications, supporting the broader view of a “male disadvantage” that is more intricate than initially assumed. They also examined potential mechanisms that might explain the development of sex differences in fetoplacental function. In conclusion, they emphasized the need to bridge gaps in the development of appropriate diagnostic tests to predict sex-related obstetric conditions.

The primary strength of this study is that it encompasses a larger number of patients compared to most single-center trials detailed in the literature. Additionally, it represents the pioneering research examining the relationship between dual-screening biochemical parameters and both fetal weight and gender. The limitations of this investigation include its retrospective nature, lack of comparison, and representation of results from single-center data.

Conclusions

Pregnancies with low PAPP-A levels during the first-trimester screening should be thoroughly monitored due to the risk of IUGR. It has been found that PAPP-A levels are lower in boys than in girls. Consequently, male infants may bear a greater risk of poor obstetric outcomes than female infants. However, additional research, especially multicenter, prospective studies, is needed to corroborate these conclusions.

References

1. Abbara A, Al-Memar M, Phylactou M, Daniels E, Patel B, Eng PC, et al. Changes in Circulating Kisspeptin Levels During Each Trimester in Women With Antenatal Complications. J Clin Endocrinol Metab. 2022 Jan 1;107(1):e71-e83. doi: 10.1210/clinem/dgab617. PMID: 34427658; PMCID: PMC8684464.
2. Abaci Turk E, YunHJ, Feldman HA, Lee JY, Lee HJ, Bibbo C, et al. Association between placental oxygen transport and fetal brain cortical development: a study in monochorionic diamniotic twins. Cereb Cortex. 2024 Jan 14;34(1):bhad383. doi: 10.1093/cercor/bhad383. PMID: 37885155; PMCID: PMC11032198.
3. Movahedi M, Farahbod F, Zarean E, Hajihashemi M, Haghollahi F, Farahmand M. Evaluation of Fetal and Maternal Outcomes in Chorion Villus Sampling (CVS). Adv Biomed Res. 2023 May 19;12:133. doi: 10.4103/abr.abr_229_22. PMID: 37434920; PMCID: PMC10331521.
4. Dias da Silva C, Sarmento Gonçalves I, Ramalho C. Association of low pregnancy associated plasma protein-A with increased umbilical artery pulsatility index in cases of fetal weight between the 3rd and 10th percentiles: a retrospective cohort study. J Perinat Med. 2023 Oct 20;52(1):90-5. doi: 10.1515/jpm-2023-0156. PMID: 37853809.
5. Turrado Sánchez EM, De Miguel Sánchez V, Macía Cortiñas M. Correlation Between PAPP-A Levels Determined During the First Trimester and Birth Weight at Full-Term. Reprod Sci. 2023 Nov;30(11):3235-42. doi: 10.1007/s43032-023-01270-4. Epub 2023 May 26. PMID: 37237249; PMCID: PMC10643350.
6. Tsibizova V, Al-Sannan B, Fedorova A, Govorov I, Meyyazhagan A, Di Renzo GC. Can we improve the outcome of pregnancies with low serum PAPP-A in the first trimester? J Matern Fetal Neonatal Med. 2024 Dec;37(1):2326303. doi: 10.1080/14767058.2024.2326303. Epub 2024 Mar 19. PMID: 38503546.
7. Conover CA, Oxvig C. The Pregnancy-Associated Plasma Protein-A (PAPP-A) Story. Endocr Rev. 2023 Nov 9;44(6):1012-28. doi: 10.1210/endrev/bnad017. PMID: 37267421.
8. Prasad P, Romero R, Chaiworapongsa T, Gomez-Lopez N, Lo A, Galaz J, et al. Further Evidence that an Episode of Premature Labor Is a Pathologic State: Involvement of the Insulin-Like Growth Factor System. Fetal Diagn Ther. 2023;50(4):236-47. doi: 10.1159/000530862. Epub 2023 May 10. PMID: 37231893; PMCID: PMC10591834.
9. Davenport BN, Wilson RL, Jones HN. Interventions for placental insufficiency and fetal growth restriction. Placenta. 2022 Jul;125:4-9. doi: 10.1016/j.placenta.2022.03.127. Epub 2022 Apr 4. PMID: 35414477; PMCID: PMC10947607.
10. Hord TK, Tanner AR, Kennedy VC, Lynch CS, Winger QA, Rozance PJ, et al. Impact of Chorionic Somatomammotropin In Vivo RNA Interference Phenotype on Uteroplacental Expression of the IGF Axis. Life (Basel). 2023 May 26;13(6):1261. doi: 10.3390/life13061261. PMID: 37374044; PMCID: PMC10302269.
11. Dal Y, Akkuş F, Karagün Ş, Nessar AZ, Karaca SG, Coşkun A. The role of second trimester uterine artery Doppler in predicting obstetric and neonatal outcomes in abnormal first-trimester maternal serum pregnancy-associated plasma protein-A and free β-human chorionic gonadotropin values. J Clin Ultrasound. 2024 Feb 14. doi: 10.1002/jcu.23644. Epub ahead of print. PMID: 38353146.
12. Liu J, Zhang X, Yu Z, Zhang T. Exosomes Promote Atherosclerosis Progression by Regulating Circ_100696/miR-503-5p/PAPPA Axis-Mediated Vascular Smooth Muscle Cells Proliferation and Migration. Int Heart J. 2023;64(5):918-27. doi: 10.1536/ihj.23-089. PMID: 37778995.
13. Buhimschi IA, Zhao G, El Helou Y, Frye LJ, Winikoff B, Raymond EG. Analytical Comparison of Pregnancy-Associated Plasma Protein-A (PAPP-A) Immunoassays for Biochemical Determination of Gestational Age. J Appl Lab Med. 2021 Nov 1;6(6):1517-32. doi: 10.1093/jalm/jfab057. PMID: 34329446.
14. Caron L, Fillion A, Giguère Y, Audibert F, Forest JC, Gasse C, Girard M, Laforest G, Guerby P, Bujold E. First-trimester screening for Down syndrome using quadruple maternal biochemical markers. Clin Chem Lab Med. 2023 Mar 29;61(9):1630-5. doi: 10.1515/cclm-2022-1305. PMID: 36989429.
15. Kane D, D’Alton ME, Malone FD. Rare chromosomal abnormalities: Can they be identified using conventional first trimester combined screening methods? Eur J Obstet Gynecol Reprod Biol X. 2021 Feb 27;10:100123. doi: 10.1016/j.eurox.2021.100123. PMID: 33733087; PMCID: PMC7937980.
16. Parry S, Carper BA, Grobman WA, Wapner RJ, Chung JH, Haas DM, et al. Placental protein levels in maternal serum are associated with adverse pregnancy outcomes in nulliparous patients. Am J Obstet Gynecol. 2022 Sep;227(3):497. e1-497.e13. doi: 10.1016/j.ajog.2022.03.064. Epub 2022 Apr 26. PMID: 35487327; PMCID: PMC9420814.
17. Kantomaa T, Vääräsmäki M, Gissler M, Sairanen M, Nevalainen J. First trimester low maternal serum pregnancy associated plasma protein-A (PAPP-A) as a screening method for adverse pregnancy outcomes. J Perinat Med. 2022 Sep 23;51(4):500-9. doi: 10.1515/jpm-2022-0241. PMID: 36131518.
18. Sovio U, Gaccioli F, Cook E, Charnock-Jones DS, Smith GCS. Association between adverse pregnancy outcome and placental biomarkers in the first trimester: A prospective cohort study. BJOG. 2024 May;131(6):823-31. doi: 10.1111/1471-0528.17691. Epub 2023 Oct 12. PMID: 37822261.
19. Kapustin RV, Kascheeva TK, Alekseenkova EN, Shelaeva EV. Are the first-trimester levels of PAPP-A and fß-HCG predictors for obstetrical complications in diabetic pregnancy? J Matern Fetal Neonatal Med. 2022 Mar;35(6):1113-9. doi: 10.1080/14767058.2020.1743658. Epub 2020 Mar 30. PMID: 32228094.
20. Huang T, Bellai-Dussault K, Meng L, Hull D, Howley H, Reszel J, et al. First and second trimester maternal serum markers for prenatal aneuploidy screening: An update on the adjustment factors for race, smoking, and insulin dependent diabetes mellitus. Clin Biochem. 2023 Aug; 118:110596. doi: 10.1016/j.clinbiochem.2023.110596. Epub 2023 Jun 8. PMID: 37295638.
21. Caron L, Ghesquiere L, Bujold E. Pregnancy associated plasma protein-A for the prediction of small for gestational age. J Perinat Med. 2023 Jan 2;51(5):718-9. doi: 10.1515/jpm-2022-0545. PMID: 36584324.
22. Cokmez H, Yozgat ST. The effect of fetal gender on the biochemical markers of the first-trimester screening. Saudi Med J. 2022 Apr;43(4):348-52. doi: 10.15537/smj.2022.43.4.20210906. PMID: 35414612; PMCID: PMC9998053.
23. Spencer K, Ong CY, Liao AW, Papademetriou D, Nicolaides KH. The influence of fetal sex in screening for trisomy 21 by fetal nuchal translucency, maternal serum free β-hCG and PAPP-A at 10–14 weeks of gestation. Prenatal diagnosis. 2000;20(8):673-5.
24. Cowans NJ, Stamatopoulou A, Maiz N, Spencer K, Nicolaides KH. The impact of fetal gender on first trimester nuchal translucency and maternal serum free β-hCG and PAPP-A MoM in normal and trisomy 21 pregnancies. Prenatal Diagnosis. 2009;29(6):578-81.
25. Stark MJ, Dierkx L, Clifton VL, Wright IM. Alterations in the maternal peripheral microvascular response in pregnancies complicated by preeclampsia and the impact of

fetal sex. The Journal of the Society for Gynecologic Investigation: JSGI. 2006;13:573-8.
26. Broere-Brown ZA, Schalekamp-Timmermans S, Hofman A, Jaddoe VWV, Steegers EAP. Fetal sex dependency of maternal vascular adaptation to pregnancy: a prospective population-based cohort study. BJOG. 2016;123(7):1087-95.
27. Inkster AM, Fernández-Boyano I, Robinson WP. Sex Differences Are Here to Stay: Relevance to Prenatal Care. J Clin Med. 2021 Jul 5;10(13):3000. doi: 10.3390/jcm10133000. PMID: 34279482; PMCID: PMC8268816.

J Surg Med. 2025;9(7):98-103.
https://doi.org/10.28982/josam.8268

JOSAM

Research article
https://jsurgmed.com/

Journal of Surgery and Medicine

e-ISSN: 2602-2079

Stacked hybrid model: Multi-layer perceptron and logistic regression with meta-learning for cesarean section classification

Emre Yalçın [1], Hayriye Tanyıldız [2], Serpil Aslan [3], Süleyman Cansun Demir [1], Mesut Avan [1], Fatma İşlek Uzay [1], Serdar Aykut [1]

[1] Department of Obstetrics and Gynecology, Division of Perinatology, Cukurova University School of Medicine, 01330, Adana, Turkey
[2] Department of Informatics, Malatya Turgut Ozal University, 44210 Malatya, Turkey
[3] Department of Software Engineering, Faculty of Engineering and Natural Sciences, Malatya Turgut Ozal University, 44210, Malatya, Turkey

ORCID of the author(s)

EY: https://orcid.org/0000-0001-7088-6749
HT: https://orcid.org/0000-0002-6300-9016
SA: https://orcid.org/0000-0001-8009-063X
SCD: https://orcid.org/0000-0001-8331-9559
MA: https://orcid.org/0009-0001-8458-6963
FİU: https://orcid.org/0000-0002-8660-4854
SA: https://orcid.org/0000-0002-6590-9982

Corresponding Author
Emre Yalçın
Department of Obstetrics and Gynecology, Division of Perinatology, Cukurova University School of Medicine, 01330, Adana, Turkey
E-mail: dremreyalcin23@gmail.com

Ethics Committee Approval
This study was carried out using the publicly available and anonymized "Caesarian Section Classification Data Set" taken from kaggle.com. As the dataset does not include personal data or involve direct human participation, ethics committee approval was not required. Furthermore, no additional permissions or ethical approvals were necessary for its use.

Conflict of Interest
No conflict of interest was declared by the authors.

Financial Disclosure
The authors declared that this study has received no financial support.

Published
2025 July 4

Abstract

Background/Aim: This study aims to develop an interpretable and practical decision support method for early prediction of the need for cesarean delivery. Although machine learning and deep learning models are prevalent in the literature, their generalization capabilities are often restricted, especially when utilizing small clinical datasets. This limitation underscores the necessity for robust, transparent, and well-regularized models in medical decision-making processes.

Methods: The study proposed a stacking-based hybrid model, which combines the strengths of both classical and modern techniques. The data were normalized using StandardScaler, and feature selection involved principal component analysis (PCA) and SelectKBest to capture global and target-relevant patterns. In the classification phase, two parallel learners – a regularized multi-layer perceptron (MLP) and logistic regression – were used, followed by a random forest meta-learner.

Results: The experimental analysis demonstrated that the proposed model achieved an average accuracy of 96.43% under stratified 5-fold cross-validation. Although this result surpassed the performance of other baseline models within the dataset, it should be regarded as preliminary due to the limited sample size.

Conclusion: The findings indicate that the proposed hybrid approach has potential as a promising direction for future clinical decision support research. Nonetheless, additional validation using larger and more diverse datasets is necessary to adequately assess its generalizability and practical utility.

Keywords: cesarean prediction, clinical decision support, medical data analysis, machine learning in healthcare

How to cite: Yalçın E, Tanyıldız H, Aslan S, Demir SC, Avan M, İşlek Uzay F, Aykut S. Stacked hybrid model: Multi-layer perceptron and logistic regression with meta-learning for cesarean section classification. J Surg Med. 2025;9(7):98-103.

Introduction

The global rate of cesarean deliveries has significantly increased in recent decades. The World Health Organization (WHO) recommends a cesarean section (CS) rate between 10% and 15%; however, many countries have far exceeded this recommendation. For example, before the 1980s, CS rates were generally below 10%, but in the past decade, they have surpassed 30% in many developed countries [1]. Although cesarean delivery is essential when medically justified, its unnecessary use can lead to various complications, prolonged recovery times, and increased burdens on healthcare systems.

Currently, no standardized method supports clinical teams in making objective decisions about CSs in borderline cases with unclear medical indications [2]. In response, artificial intelligence (AI)-based systems have gained traction in medicine, notably for classification tasks. In obstetrics, predictive models for CS can assist clinicians in decision-making. However, challenges such as small sample sizes, class imbalance, clinical data complexity, and the need for interpretability hinder the development of effective models.

To address these limitations, this study proposes a novel stacking-based hybrid classification model for CS prediction. This model integrates classical machine learning algorithms – such as logistic regression, decision trees, and support vector machines – with modern deep learning architectures, including multi-layer perceptron (MLP), convolutional neural network (CNN), and long short-term memory (LSTM). The goal is to leverage both the interpretability of traditional methods and the high representation power of deep learning. Based on experimental observations, a meta-learning approach was employed to harness the strengths of the individual models.

The proposed framework incorporates a feature fusion strategy that integrates principal component analysis (PCA) with SelectKBest. This combination retains global variance and target-specific relevance, thereby reducing overfitting in small clinical datasets. The classification structure utilizes a regularized MLP and logistic regression as base learners, whose outputs are subsequently fed into a random forest meta-learner. This layered design enhances generalization by capturing both linear and non-linear patterns effectively.

Compared to the single-model approaches commonly found in the literature, the proposed hybrid model achieved a superior accuracy of 96.43%, demonstrating its effectiveness in CS classification. The logistic regression component of the model enhances interpretability, thus supporting both practical clinical utility and academic relevance.

Furthermore, this study addresses a gap in the literature by introducing an integrated model that combines stacking, dimensionality reduction, and ensemble learning techniques specifically tailored for cesarean prediction. Although previous studies [3-5] have investigated various feature selection and classification algorithms, few have successfully integrated multiple advanced techniques into a single architecture with demonstrated clinical applicability.

Materials and methods

Dataset and pre-processing

The dataset used in this study was sourced from a publicly available resource on Kaggle [6]. It comprises 26 instances, covering both cesarean and non-cesarean deliveries. Each record encompasses various maternal and fetal attributes, including maternal age, blood pressure, fetal heart rate, and prior delivery history. The target variable specifies whether the delivery was a CS or occurred naturally.

The dataset comprises six input features alongside a binary target variable. The features are defined as follows: Age (represents the mother's age in years, ranging from 22 to 40); Delivery Number (Indicates the total number of previous deliveries, recorded numerically and ranging from 1 to 4); Delivery Time (an ordinal value that specifies the timing of birth, with three categories: 1 for timely, 2 for late, and 3 for early); Blood Pressure (a categorical value representing blood pressure status, where 1 denotes low, 2 normal, and 3 high); Heart Problem (a binary indicator of the presence of a maternal heart condition, coded as 0 for absence and 1 for presence); and Target (Cesarean) (a binary outcome variable that indicates the mode of delivery, where 1 represents a CS and 0 denotes a natural delivery).

Among the 26 cases, 15 were cesarean deliveries and 11 were natural births, which reflects a mildly imbalanced class distribution. Most participants had normal blood pressure and no heart problems, and the majority were first-time mothers. This information is included to enhance transparency about the dataset structure and to enable a more informed assessment of potential biases.

In the pre-processing phase, normalization was applied to standardize feature scales, and incomplete records were removed to ensure data quality. To enhance classification performance, feature selection techniques were utilized. Specifically, PCA and SelectKBest based on the ANOVA F-score were employed. This combined approach reduced dimensionality, eliminated irrelevant or noisy features, and preserved the most informative attributes for model training.

Machine learning models

Logistic regression is a widely used linear classification method for binary problems. It employs the logistic (sigmoid) function to predict the probabilities of the dependent variable, yielding outputs between 0 and 1. Due to its high interpretability, logistic regression is particularly favored in fields such as healthcare, finance, and social sciences [7].

The random forest is an ensemble learning method composed of multiple decision trees. Each tree is trained on a distinct subset of data with randomly selected features. This approach allows random forests to outperform single decision trees in terms of accuracy and generalization, owing to their diversity. Additionally, random forests significantly reduce the risk of overfitting. The algorithm yields effective results in both classification and regression tasks, making it particularly useful for large datasets. A further advantage of random forests is their capability to produce interpretable outputs, such as feature importance rankings, which are valuable to researchers seeking to understand model predictions [8]. However, models with a large number of trees can experience increased training time and computational costs.

Deep learning models

The multi-layer perceptron (MLP): MLP is one of the most fundamental and widely utilized types of artificial neural networks, primarily used for supervised learning tasks [9]. As a feedforward neural network, an MLP typically consists of an input layer, one or more hidden layers, and an output layer. Each neuron is fully connected to neurons in the preceding and following layers. The use of non-linear activation functions enables the model to learn complex mappings. Variants, including residual MLPs, batch-normalized MLPs, and deeper architectures, are often employed to enhance learning performance and ensure training stability.

Convolutional neural networks (CNNs): CNNs originally developed for image processing tasks, have recently gained popularity in analyzing one-dimensional time series data. By utilizing 1D convolutional layers, CNNs can automatically detect local patterns and short-term dependencies, such as trends or periodic signals, within sequential data. This capability renders them suitable for applications in fields including financial forecasting, sensor signal analysis, and clinical time series interpretation. Compared to traditional statistical methods like ARIMA or standard machine learning algorithms, CNNs often provide superior feature extraction capabilities and exhibit higher predictive performance in many cases [10].

Long short-term memory (LSTM): LSTM networks are a type of recurrent neural network (RNN) designed to model long-range dependencies in sequential data [11]. Distinct from traditional RNNs, LSTMs incorporate memory cells and gating mechanisms – specifically input, forget, and output gates – that maintain information over extended periods and address the vanishing gradient problem. This architecture allows LSTMs to retain relevant patterns from earlier time steps, making them particularly suitable for tasks such as language modeling, energy consumption prediction, and financial time series forecasting.

Figure 1: The architecture of the proposed model.

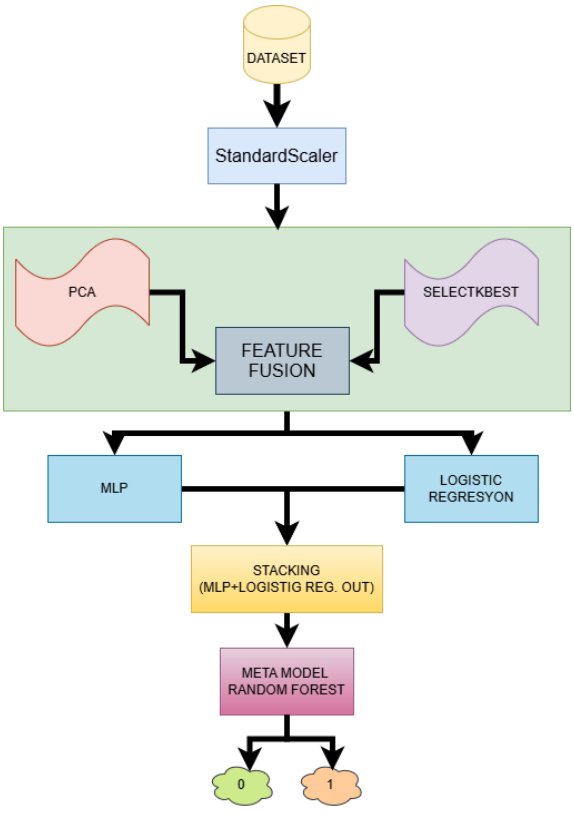

The proposed hybrid model

The hybrid model developed in this study aims to enhance classification performance by integrating deep learning with traditional machine learning methods. Figure 1 presents the model's overall architecture. It is structured around a multi-stage pre-processing pipeline that optimizes the feature space before model training.

In the initial stage, data normalization is executed using StandardScaler. This ensures that features on varying scales equitably contribute to the learning process. Subsequently, dimensionality reduction is achieved through a feature fusion strategy that integrates PCA with SelectKBest based on the ANOVA F-score. PCA identifies new orthogonal components that maximize variance, while SelectKBest retains statistically significant original features correlated with the target variable. By combining these approaches, the model efficiently captures both global and local patterns, focusing on the most informative attributes and improving learning efficiency.

After feature selection, the dataset is simultaneously processed through two distinct classifiers. The first classifier is a deep neural network, constructed with a multi-layered architecture and equipped with regularization techniques such as L2 regularization, dropout, batch normalization, and the LeakyReLU activation function. This network is designed to capture complex, non-linear relationships within the data. In parallel, a logistic regression model is trained, offering a simpler, interpretable alternative that excels at learning linear decision boundaries and provides transparency in clinical contexts.

The final and most innovative component of the proposed system is the meta-learning stage, which utilizes the stacking ensemble method. In this stage, the output probabilities from both the deep neural network and logistic regression model are regarded as a new feature space. These outputs are then input into a random forest meta-classifier, which generates the final predictions. This ensemble approach capitalizes on the strengths of both base learners, thereby enhancing the model's generalization capability.

Results

To evaluate the performance of the proposed model and baseline algorithms, we conducted a series of experiments in the Google Colab Pro environment, which features an NVIDIA A100 GPU and 84 GB of RAM. The implementations were executed using the Python programming language. In this study, model performance was assessed using two key metrics: accuracy, which measures overall classification success, and specificity, which indicates the model's ability to correctly identify non-cesarean cases. These metrics were selected for their relevance in evaluating both general effectiveness and clinical reliability. Given the small sample size and class imbalance in the dataset, we employed stratified 5-fold cross-validation to ensure balanced representation of classes in each fold. The dataset was divided into five subsets for each iteration; four were used for training and one for testing. Performance results were averaged across all folds to derive a robust and generalizable estimate of model effectiveness.

Among deep learning models, the Simple MLP achieved the highest overall accuracy, reaching 85.71%. The Residual MLP demonstrated superior specificity at 88.24%, highlighting its

effectiveness in correctly identifying non-cesarean cases. The CNN model also performed well, showing balanced results across accuracy and specificity. In contrast, MLP variants using batch normalization or dropout exhibited weaker performance, especially in specificity, suggesting that such regularization techniques may be less effective in small-sample clinical settings.

Table 1: The performance comparisons of the deep learning models.

Deep Models	Accuracy	Specificity
Simple MLP	85.71	35.29
Deep MLP	75	64.71
MLP with Dropout	60.71	35.29
MLP with Batch Normalization	57.14	29.41
MLP with Residual Connections	78.57	88.24
CNN	82.14	70.59
LSTM	67.86	47

Figure 2 offers further insight into model behavior through confusion matrix analysis. The Simple MLP achieved the highest accuracy, correctly classifying 24 out of 28 instances. The CNN and Residual MLP models followed closely, with 23 and 22 correct predictions, respectively. These models exhibited relatively balanced performance across both classes. In contrast, models such as the Dropout MLP and LSTM, while successful in identifying all cesarean cases, produced a high number of false positives for non-cesarean cases, significantly reducing their specificity. The Batch Normalized MLP demonstrated the lowest overall performance, struggling to identify non-cesarean cases and generating the most misclassifications. These observations underscore the importance of both architecture and regularization in achieving balanced performance. Although deep learning models can achieve high predictive accuracy, their class-wise reliability varies considerably based on design choices.

Figure 2: Confusion matrices for each model architecture: (a) Simple MLP representing a basic multilayer perceptron structure; (b) Deep MLP with increased depth; (c) MLP with Dropout regularization; (d) MLP with Batch Normalization to stabilize learning; (e) MLP with Residual Connections to mitigate vanishing gradient issues; (f) Convolutional Neural Network (CNN) specialized for spatial data; (g) Long Short-Term Memory (LSTM) network tailored for sequential data.

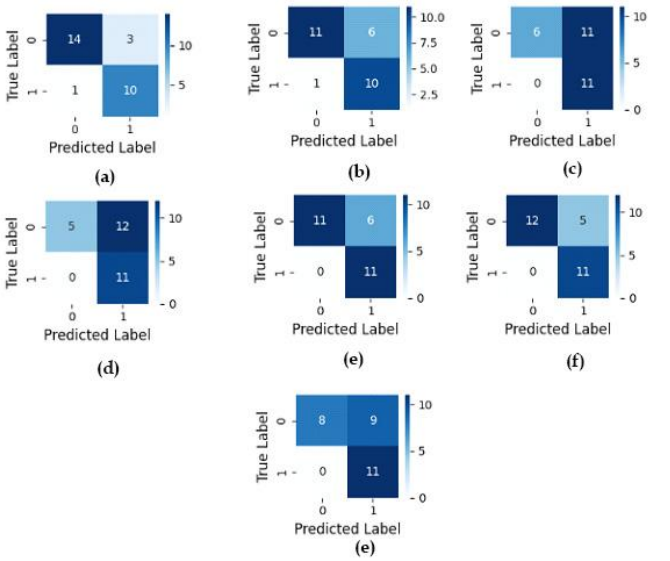

The experimental results of the proposed model

In the proposed model, feature selection for the Deep MLP architecture occurred in two stages: PCA and SelectKBest based on ANOVA F-values. This pre-processing step aimed to reduce dimensionality, eliminate irrelevant features, and enhance the model's learning efficiency. By retaining the most significant variables, we expected the model to achieve improved generalization and predictive performance. The experimental results of this model, developed using the optimized feature set, are presented in the following section.

Figure 3 summarizes the stepwise improvements observed in the proposed model. In the first stage, feature selection using PCA and SelectKBest enhanced the Deep MLP's ability to distinguish between classes. In the second stage, incorporating logistic regression as a meta-learner further improved class-wise balance and overall prediction consistency. This approach resulted in the best-performing hybrid configuration.

Figure 3: Confusion matrices of the proposed hybrid models: (a) Deep MLP with PCA and SelectKBest (ANOVA F-value) feature selection; (b) Hybrid model integrating Logistic Regression into the selected feature structure.

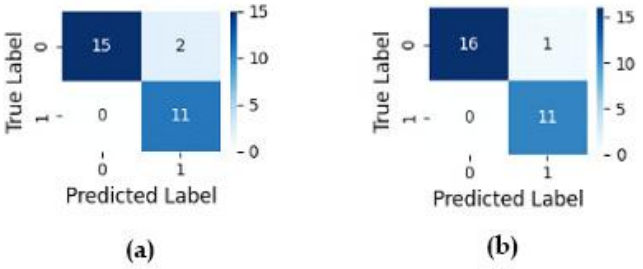

Table 2 presents a comparison between the Deep MLP model after feature selection and the final hybrid model that integrates logistic regression. Feature selection led to substantial performance enhancements, and the hybrid design further improved both accuracy and specificity. The proposed model achieved the best overall results, particularly in accurately identifying non-cesarean cases. These findings suggest that integrating deep learning with a classical learner in a feature-optimized architecture can greatly enhance predictive performance and class-level reliability in limited clinical datasets.

Table 2: Performance comparison of the Deep MLP model with feature selection and the proposed hybrid model integrating logistic regression.

Deep Model	Accuracy	Specificity
(PCA - SelectKBest) + MLP	92.86	88.24
((PCA - SelectKBest) + MLP + Logistic Regression)	96	94.12

Discussion

This study's primary contribution is the development of a novel hybrid model that combines deep learning and traditional machine learning approaches to address the clinically significant and sensitive task of categorizing cesarean deliveries. Previous studies [3-5,12,13] have employed various algorithms individually, achieving accuracy rates between 63% and 89%. In contrast, our proposed model achieves an accuracy of 96.43%, surpassing all existing approaches. By incorporating dimensionality reduction and feature selection techniques, such as PCA and SelectKBest, the model focuses on the most informative inputs, thereby accelerating the training process and reducing the risk of overfitting. While the Deep MLP model is highly capable of learning complex relationships, the logistic regression model enhances interpretability and simplicity in the decision-making process. The stacking architecture, which integrates the outputs of both models using a random forest classifier, effectively harnesses the strengths of each component to enhance overall performance.

Figure 4 compares the accuracy metrics of the proposed hybrid model with various machine learning models (DT, LG, RF, SVM, KNN) and deep learning models (Simple MLP, CNN, LSTM, Residual MLP, etc.). The graph shows that traditional models such as SVM, KNN, and Decision Tree achieved accuracy rates below 50%. Among the deep learning models, only the

Figure 4: Comparison of accuracy rates achieved by the proposed hybrid model and other traditional machine learning (DT, LG, RF, SVM, KNN) and deep learning models (Simple MLP, CNN, LSTM, Residual MLP).

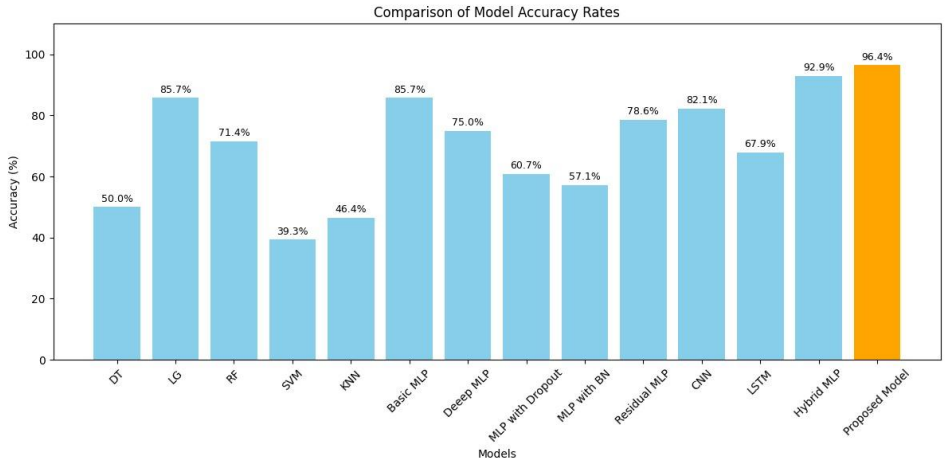

Simple MLP and CNN surpassed 80%. Notably, the proposed hybrid model outperformed all others with an accuracy of 96%. These findings suggest that the proposed model is highly reliable and suitable for integration into clinical decision support systems, especially in critical tasks such as cesarean classification.

Despite the promising performance of the proposed hybrid model, it is crucial to note that the dataset used in this study consisted of only 26 instances. This limited sample size inherently restricts the model's ability to generalize and heightens the risk of overfitting, particularly with the use of complex architectures like deep neural networks. Employing deep learning techniques on such a small dataset may be methodologically questionable due to their tendency to memorize rather than generalize in data-scarce environments. Although various regularization and ensemble techniques were implemented to address these concerns, the results should be viewed as preliminary proof-of-concept. This study aimed to explore whether a hybrid structure, combining interpretability with complexity, could still provide meaningful predictive insights under the real-world limitations often encountered in clinical practice. Further research with larger and more diverse datasets is necessary to confirm the robustness and applicability of the proposed approach.

Study limitations

The primary limitation of this study is the small dataset size (n=26), which diminishes statistical power and limits the generalizability of the findings. Despite using regularization techniques and feature optimization to construct the hybrid model and reduce overfitting, the small sample size presents a significant obstacle to effective model validation. Additionally, applying feature selection methods such as PCA and SelectKBest to such a constrained dataset can produce unstable results, as the identified patterns may not accurately reflect broader population dynamics. Furthermore, although stacking ensemble learning was employed to improve predictive performance, training both the base and meta-learners on the same limited dataset increases the risk of overfitting to sample-specific noise.

Despite implementing various control measures, including dimensionality reduction and regularization strategies, the outcomes should be considered preliminary. This study is best regarded as a feasibility analysis rather than a definitive modeling framework. Future research should aim to validate the approach using larger, multicenter datasets to ensure broader clinical applicability and reliability.

Conclusion

In this study, widely used machine learning and deep learning approaches for predicting the likelihood of cesarean delivery were systematically evaluated. A stacking-based hybrid model was proposed, combining the most effective aspects of these approaches. By applying PCA and SelectKBest, meaningful features were extracted, which both accelerated the learning process and enabled the model to capture complex relationships. The model's multi-stage structure not only aligns with the nature of medical diagnostic problems but also outperforms previous studies in the literature, achieving an accuracy rate of 96.43%.

In conclusion, the proposed hybrid model shows significant potential as a clinical decision support tool. It may be adapted for real-time applications by testing on broader and more diverse datasets. Future studies should focus on integrating explainable AI (XAI) techniques to improve the clinical interpretability of model outputs and facilitate their integration with expert systems.

References

1. Afroja S, Kabir MA, Saleh AB. Machine learning-based algorithms for determining C-section among mothers in Bangladesh. Int J Travel Med Glob Health. 2023;11(4):391-401. doi: 10.34172/ijtmgh.2023.65.
2. Chu K, Cortier H, Maldonado F, Mashant T, Ford N, Trelles M. Cesarean section rates and indications in sub-Saharan Africa: a multi-country study from Médecins Sans Frontières. PLoS One. 2012;7(9):e44484. doi: 10.1371/journal.pone.0044484.
3. Desyani T, Saifudin A, Yulianti Y. Feature selection based on Naive Bayes for caesarean section prediction. IOP Conf Ser Mater Sci Eng. 2020;879(1):012091. doi: 10.1088/1757-899X/879/1/012091
4. de Souza HC, Perdoná GS, Marcolin AC, Oyeneyin LO, Oladapo OT, Mugerwa K, et al. Development of caesarean section prediction models: secondary analysis of a prospective cohort study in two sub-Saharan African countries. Reprod Health. 2019;16:1-11. doi: 10.1186/s12978-019-0832-4.
5. Pereira S, Portela F, Santos MF, Machado J, Abelha A. Predicting type of delivery by identification of obstetric risk factors through data mining. Procedia Comput Sci. 2015;64:601-9. doi: 10.1016/j.procs.2015.08.572.
6. Amir75. Caesarean Section Classification Dataset [Internet]. Kaggle; [cited 2025 April 14]. Available from: https://www.kaggle.com/datasets/amir75/caesarean-section-classification/data
7. Hosmer DW Jr, Lemeshow S, Sturdivant RX. Applied Logistic Regression. 3rd ed. Hoboken (NJ): John Wiley & Sons; 2013.
8. Rigatti SJ. Random forest. Journal of Insurance Medicine. 2017;47(1):31-9.
9. Desai M, Shah M. An anatomization on breast cancer detection and diagnosis employing multi-layer perceptron neural network (MLP) and convolutional neural network (CNN). Clin eHealth. 2021;4:1-11. doi: 10.1016/j.ceh.2020.12.001
10. Toğaçar M, Ergen B. Processing 2D barcode data with metaheuristic based CNN models and detection of malicious PDF files. Appl Soft Comput. 2024;161:111722. doi: 10.1016/j.asoc.2023.111722
11. Hochreiter S, Schmidhuber J. Long short-term memory. Neural Comput. 1997;9(8):1735-80. doi: 10.1162/neco.1997.9.8.1735
12. Khan NI, Mahmud T, Islam MN, Mustafina SN. Prediction of cesarean childbirth using ensemble machine learning methods. In: Proceedings of the 22nd International

Conference on Information Integration and Web-based Applications & Services; 2020 Nov; pp. 331-339. doi: 10.1145/3428757.3429136

13. Yimer NB, Mekonnen EG. Development and validation of a risk prediction model for caesarean delivery among multiparous women. Sci Rep. 2025;15(1):5326. doi: 10.1038/s41598-025-12990-9

J Surg Med. 2025;9(7):104-108.
https://doi.org/10.28982/josam.8069

JOSAM

Journal of Surgery and Medicine

e-ISSN: 2602-2079

Research article
https://jsurgmed.com/

CDC42 and EZH2 are overexpressed in colorectal cancer: Are they minimal invasive diagnostic markers?

Tuba Denkçeken [1], Elif Onur [2], Mehmet Şahin [3], Rabia Milli [3]

[1] SANKO University, Faculty of Medicine, Department of Biophysics, Gaziantep, Turkey
[2] SANKO University, Faculty of Medicine, Department of Medical Biology, Gaziantep, Turkey
[3] Gaziantep University, Faculty of Medicine, Department of Medical Biology, Gaziantep, Turkey

ORCID of the author(s)

TD: https://orcid.org/0000-0002-4663-5410
EO: https://orcid.org/0000-0002-1690-3170
MŞ: https://orcid.org/0000-0001-8312-5156
RM: https://orcid.org/0000-0003-0246-0687

Corresponding Author
Elif Onur
SANKO University, Faculty of Medicine, Department of Medical Biology, 27090 Gaziantep, Turkey
E-mail: elif.onur@sanko.edu.tr

Ethics Committee Approval
The study was approved by the Ethics Committee of SANKO University (2019/15-01). All procedures in this study involving human participants were performed in accordance with the 1964 Helsinki Declaration and its later amendments.

Conflict of Interest
No conflict of interest was declared by the authors.

Financial Disclosure
This research was funded by TÜSEB with project grant no. TA-4614.

Published
2025 July 11

Abstract

Background/Aim: Bioinformatics methods have been used to show that cell division cycle 42 (CDC42) and enhancer of zeste homolog 2 (EZH2) have potential oncogenic effects in colorectal cancer (CRC). In this study, we performed experimental validation of these genes.
Methods: We considered the possible role of CDC42 and EZH2 genes in SW480 and SW620 cells. Furthermore, blood samples were gathered from CRC patients and healthy controls to compare CDC42 and EZH2 levels, and relative mRNA and protein levels were measured.
Results: CDC42 and EZH2 expression levels were significantly increased in the SW480 and SW620 cell lines when compared with normal CRL-1790. In addition, when we examined CDC42 and EZH2 expression levels in blood samples of 20 CRC patients and 20 healthy controls by RT-qPCR, the levels of CDC42 and EZH2 were significantly upregulated in patients with CRC compared with healthy control subjects. Similar results were obtained in terms of the protein expression levels of CDC42 and EZH2.
Conclusion: These data reveal that CDC42 and EZH2 are significantly overexpressed in CRC. Considering that high gene and protein expression levels of CDC42 and EZH2 were found in the serum of patients suffering from CRC, these two genes may be developed as minimally invasive diagnostic markers for CRC detection.

Keywords: colorectal cancer, CDC42, EZH2, noninvasive biomarker

How to cite: Denkçeken T, Onur E, Şahin M, Milli R. CDC42 and EZH2 are overexpressed in colorectal cancer: Are they minimal invasive diagnostic markers? J Surg Med. 2025;9(7):104-108.

Introduction

Colorectal cancer (CRC) is the third most commonly diagnosed cancer in the world and one of the leading causes of cancer-related deaths for both males and females [1]. Nearly 60% of patients with CRC develop metastases, which is a major cause of mortality [2]. The identification of cancer-related genes to define critical events in the development and progression of CRC is therefore extremely valuable.

Recent advances in bioinformatics analyses open up exciting new opportunities for understanding cancer genetics. Via the use of high-throughput sequencing and other technologies, scientists are now able to analyze vast amounts of genetic data, uncovering patterns, biological processes, signaling pathways, molecular functions, and relationships that were previously unknown [3,4]. In our previous study, expression profiling was downloaded from Gene Expression Omnibus (GEO) databases to determine potential biomarkers that may play an important role in CRC. Significant genes were determined via computational and bioinformatics analysis, and hub genes were verified using The Cancer Genome Atlas (TCGA) [4]. In the present study, we examined the expression and protein levels of cell division cycle 42 (CDC42) and enhancer of zeste homolog 2 (EZH2), which are among the hub genes determined to play a role in CRC.

CDC42, a member of the Rho GTPases family, is involved in the regulation of critical cellular functions. Some of those functions are cell cycle control and metastasis, rearrangement of the actin cytoskeleton, intracellular trafficking, cell fate determination, cell cycle control, cell polarity, and gene transcription [5,6]. Recently, accumulating evidence has suggested that CDC42 is highly expressed in approximately 60% of incidences in human CRCs and plays important roles in cancer development and progression [7,8]. This situation suggests a potential role of this gene in tumor development.

EZH2 is a core component of the polycomb repressor complex 2 and mediates gene silencing. EZH2 has been found to be over-expressed in many malignancies [9-12]. EZH2 downregulation can reduce growth of invasive breast carcinoma [13], tumor angiogenesis [14], and in vitro cell migration/invasion of CRC cell lines [15]. Various studies have elucidated the complex role of EZH2 in biological processes and cancer-related events.

In our study, we used RT-qPCR and enzyme-linked immunosorbent assay (ELISA) to examine the possible role of CDC42 and EZH2 gene and protein expressions in SW480 and SW620 according to the CRL-1790 cell lines. We detected that CDC42 and EZH2 were strongly upregulated in cancer cell lines relative to the control. In addition, we investigated CDC42 and EZH2 expressions in blood samples of 20 CRC patients and 20 controls, finding that they were also upregulated in circulation. These findings suggest that dysregulation of CDC42 and EZH2 expression stimulates the oncogenic potential of CRC and that they can be developed as potential diagnostic biomarkers. Based on these results, we conclude that CDC42 in blood may serve as a viable and available biomarker for CRC diagnosis and prognosis.

Materials and methods

Cell culture

CRC cell lines SW620 (metastatic), SW480 (pre-metastatic tumor), and CRL-1790 (normal colon) were purchased from the American Type Culture Collection for in vitro analysis. They were cultured in RPMI-1640 medium supplemented with 10% fetal bovine serum, 100 IU/mL penicillin, and 100μg/mL streptomycin at 37°C in a 5% humidified CO_2 atmosphere. RT-qPCR and ELISA were used to determine the expression and protein level, respectively.

Clinical samples

Human CRC blood samples (n=20) and age- and sex-matched healthy controls (n=20) were collected from SANKO University, Faculty of Medicine, Department of Gastroenterology. G-power 3.1.9.4 was utilized for sample size calculation and power analysis. Based on the difference in means between the two groups, with a significance level (α) of 0.05 and a test power (1-β) of 0.8, it was determined that the power of the test was 80% and the minimum required sample size was 7 in each group, which indicated that the number of individuals in the present study was largely sufficient to detect differential expression of genes. The patient group consisted of individuals who did not receive antitumor therapy and who had undergone colonoscopy and histopathological confirmation, while controls were those who presented to primary care outpatient clinics without gastrointestinal symptoms. This study was reviewed and approved by the Ethics Committee of SANKO University (2019/15-01). The patients and controls provided their written informed consent to participate in this study. The research was conducted according to the ethical standards of our institution and the 1964 Helsinki Declaration and its later amendments.

Real-time PCR assays

Total RNA was isolated from cells and blood samples using the Quick-RNA Miniprep Plus Kit (Zymo Research). RNA isolates concentration was checked, and 5–10 ng/μL of RNA was utilized for cDNA synthesis using specific primers. For expression analysis of CDC42 and EZH2 markers by RT-qPCR, 5 μg of the RNA samples was reverse transcribed to utilize reverse transcriptase OneScript® Plus cDNA Synthesis kit (ABM), and SYBR green-based RT-qPCR was conducted with specific primers. Relative expressions of genes were normalized to GAPDH references, and fold changes between groups were calculated using the $2^{-\Delta\Delta Ct}$ method and represented as log2 fold change [16].

ELISA

Expression of CDC42 and EZH2 marker proteins in serum obtained from CRC patients was determined by ELISA kits (Cloud-Clone). Protein concentrations in serum samples were also measured with ELISA kits.

Statistical analysis

Statistical analysis was done using RStudio. All data are presented as the means and standard deviations of three independent experiments. The t-test was used in paired group comparisons for normally distributed samples, one-way ANOVA was used in three-group comparisons, and the Mann-Whitney U test was utilized for non-normally distributed samples.

Figure 1: Flow diagram of study and patients

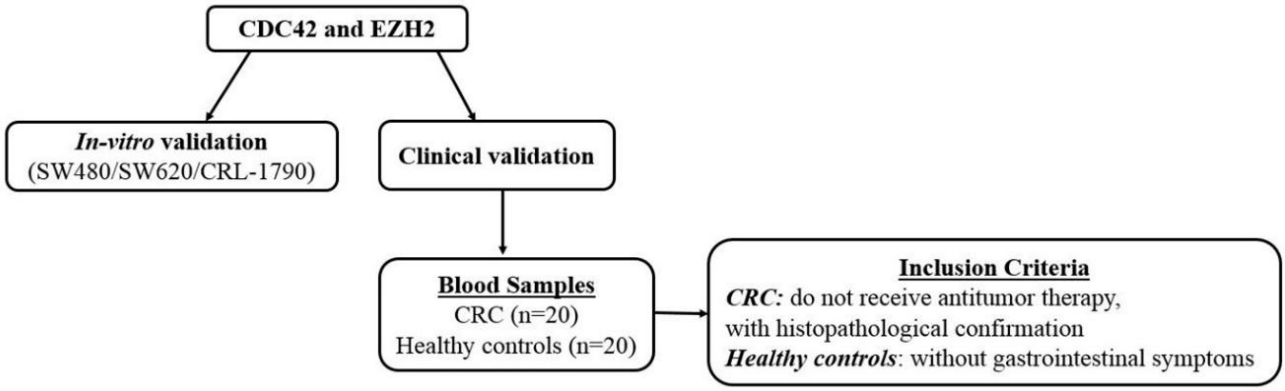

Results

The study and patient flow diagram is shown in Figure 1. CDC42 and EZH2 expression was significantly increased in the SW480 and SW620 cell lines when compared with normal CRL-1790 cells. CDC42 was expressed significantly higher in the SW620 (P=0.0011) and SW480 (P<0.0001) cell cultures (Figure 2A). EZH2 was also expressed significantly higher in the SW620 (P=0.0079) and SW480 (P=0.0073) cell cultures (Figure 2B). In addition, the CDC42 and EZH2 expression levels in the blood samples of 20 CRC patients and 20 healthy controls were also examined by RT-qPCR. The levels of CDC42 and EZH2 were significantly upregulated in patients with CRC compared with healthy control subjects. It was determined that CDC42 mRNA expression significantly increased in the CRC blood samples (P=0.0355) (Figure 3A), as did EZH2 mRNA expression (P=0.0422) (Figure 3B). Similar results were obtained in terms of the protein expression levels of CDC42 and EZH2. ELISA indicated that, compared with the healthy control, the serum CDC42 (P=0.005) and EZH2 (P=0.0004) were significantly increased in the CRC blood samples (Figure 4A–4B). These data revealed that CDC42 and EZH2 are significantly overexpressed in CRC.

Figure 2: (A) Relative CDC42 expression in CRC cell lines to CRL-1790 (three replicates per group), (B) Relative EZH2 expression in CRC cell lines to CRL-1790 (three replicates per group) by RT-qPCR (*P<0.05, ** P<0.01, ****P<0.0001).

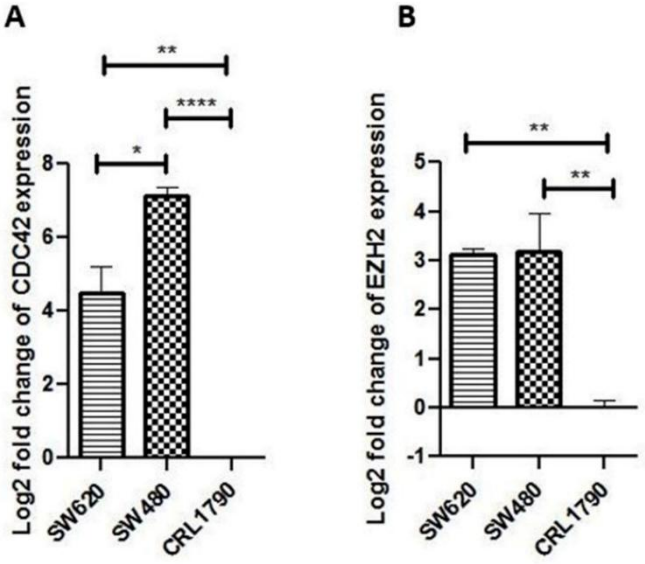

Figure 3: (A) Relative CDC42 expression in blood samples by RT-qPCR, (B) Relative EZH2 expression in blood samples by RT-qPCR (*P<0.05).

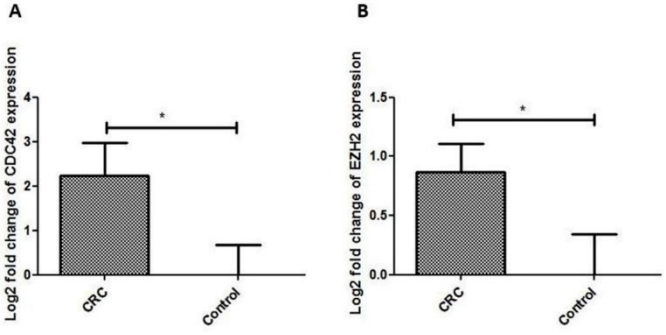

Figure 4: (A) Relative protein concentration of CDC42 in blood samples by ELISA, (B) Relative protein concentration of EZH2 in blood samples by ELISA (**P<0.01, ***P<0.001).

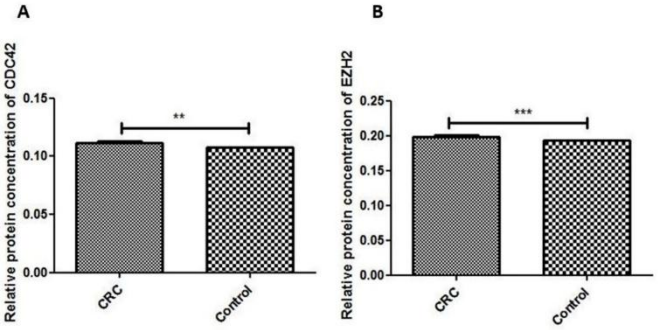

Discussion

CRC is the third most common cancer worldwide, representing the second most common cancer in women and the third most common cancer in men. There were nearly 2 million new cases of CRC in 2020 [17]. With the improvement of high-throughput sequencing and screening technologies, CRC treatment through gene-targeted therapy, which requires cancer-associated biomarker identification, has become a novel potential approach. In this study, the gene and protein expression levels of the CDC42 and EZH2 genes, which we previously determined to play a role in CRC using bioinformatics methods [4], were determined in CRC cell lines and blood samples.

CDC42 is a small GTPase involved in multiple cellular processes such as cell cycle control, gene expression, cell migration, invasion, and metastasis whose aberrant expression and activity have been shown previously in different cancer types [18,19]. Since EZH2 regulates cell cycle progression, dysregulation in EZH2 accelerates cell proliferation and prolongs cell survival. This situation can indirectly lead to carcinogenesis and cancer development. EZH2 overexpression has been identified in many cancer types [20,21]. Therapies targeting

EZH2, which is associated with multiple diseases and plays a role in several biological processes, are an important strategy in the treatment of various types of cancer and diseases.

In this study, we used two CRC cell lines and one control cell which were isolated from normal human colon tissue to investigate the expression of CDC42 and EZH2 in CRC. We found that the CDC42 and EZH2 expression levels were significantly increased in the SW480 and SW620 cell lines when compared with normal CRL-1790 cells. These results are consistent with the literature [22-24]. Interestingly, when compared to the normal cell line for both genes, much higher expression was observed in the pre-metastatic tumor cell line than in the metastatic one. The literature describes a similar situation in studies conducted with these two cell lines, where it was determined that the expression of miR-26a, miR-26b, p27, and ZNF561-AS1 in pre-metastatic cells was higher than in metastatic cells [25-27]. However, there has been no discussion about this trend. These findings suggest that these genes serve as a promoter in pre-metastatic cells and that when the cell becomes metastatic, it may transfer its function to another gene with a decrease in its expression. This also raises the possibility of CRC being diagnosed with these genes while it is still in the pre-metastatic stage. This interesting phenomenon will be evaluated in more detail in future studies.

The present study also examined CDC42 and EZH2 expression levels in blood samples of CRC patients and healthy controls. CDC42 and EZH2 were significantly overexpressed in CRC patients compared with healthy controls. Similar results were obtained in terms of the protein expression levels of CDC42 and EZH2. These data suggest that CDC42 and EZH2 act as predictive markers in CRC. In the literature, validation studies of the mentioned genes have been mostly carried out on frozen tissues or fresh tissues. The results obtained in previous studies conducted with CRC patients' tissues are compatible with the results of our study, and the expression levels of both genes have been found to be high [7,28,29]. Our literature review only identified one validation study of the CDC42 gene in blood samples [30]. The results of that study are also compatible with our results. However, no study was found investigating the EZH2 gene in the circulation of CRC patients. Considering that the present study found high expression levels of CDC42 and EZH2 in the serum of patients suffering from CRC, these two genes may be developed as minimal invasive diagnostic markers for CRC detection. To fully understand the role of CDC42 and EZH2 in CRC, a longitudinal study design with a large sample set is needed, as well as studies in mouse and cell line models. This will be a challenging but promising task.

Limitations

The main limitation of our study is that it included a single ethnicity and a small number of participants. Our findings thus need to be supported by larger studies. Despite these limitations, this study is still an important preliminary step and provides the basis for future research.

Conclusion

In conclusion, CDC42 and EZH2 were found to be upregulated in CRC. Our findings also suggest that these genes may play a diagnostic role as novel biomarkers in CRC.

References

1. Bray F, Ferlay J, Soerjomataram I, Siegel RL, Torre LA, Jemal A. Global cancer statistics 2018: GLOBOCAN estimates of incidence and mortality worldwide for 36 cancers in 185 countries. CA Cancer J Clin. 2018;68(6):394-424.
2. Rasool S, Kadla SA, Rasool V, Ganai BA. A comparative overview of general risk factors associated with the incidence of colorectal cancer. Tumor biol. 2013;34(5):2469-76.
3. Slattery ML, Herrick JS, Mullany LE, Samowitz WS, Sevens JR, Sakoda L, et al. The co-regulatory networks of tumor suppressor genes, oncogenes, and miRNAs in colorectal cancer. Genes Chromosomes Cancer. 2017;56(11):769-87.
4. Onur E, Denkçeken T. Integrative analysis of molecular genetic targets and pathways in colorectal cancer through screening large-scale microarray data. Int J Data Min Bioin. 2021;26(1-2):81-98.
5. Braga VM, Yap AS. The challenges of abundance: epithelial junctions and small GTPase signalling. Curr Opin Cell Biol. 2005;17(5):466-74.
6. Gómez del Pulgar T, Benitah SA, Valerón PF, Espina C, Lacal JC. Rho GTPase expression in tumourigenesis: evidence for a significant link. Bioessays. 2005;27(6):602-13.
7. Gómez Del Pulgar T, Valdés-Mora F, Bandrés E, Pérez-Palacios R, Espina C, Cejas P, et al. Cdc42 is highly expressed in colorectal adenocarcinoma and downregulates ID4 through an epigenetic mechanism. Int J Oncol. 2008;33(1):185-93.
8. Sakamori R, Yu S, Zhang X, Hoffman A, Sun J, Das S, et al. CDC42 inhibition suppresses progression of incipient intestinal tumors. Cancer Res. 2014;74(19):5480-92.
9. van Leenders GJ, Dukers D, Hessels D, van den Kieboom SW, Hulsbergen CA, Witjes JA, et al. Polycomb-group oncogenes EZH2, BMI1, and RING1 are overexpressed in prostate cancer with adverse pathologic and clinical features. Eur Urol. 2007;52(2):455-63.
10. Yamada A, Fujii S, Daiko H, Nishimura M, Chiba T, Ochiai A. Aberrant expression of EZH2 is associated with a poor outcome and P53 alteration in squamous cell carcinoma of the esophagus. Int J Oncol. 2011;38(2):345-53.
11. He LJ, Cai MY, Xu GL, Li JJ, Weng ZJ, Xu DZ, et al. Prognostic significance of overexpression of EZH2 and H3k27me3 proteins in gastric cancer. Asian Pac J Cancer Prev. 2012;13(7):3173-8.
12. Huqun, Ishikawa R, Zhang J, Miyazawa H, Goto Y, Shimizu Y, et al. Enhancer of zeste homolog 2 is a novel prognostic biomarker in nonsmall cell lung cancer. Cancer. 2012;118(6):1599-606.
13. Gonzalez ME, Li X, Toy K, DuPrie M, Ventura AC, Banerjee M, et al. Downregulation of EZH2 decreases growth of estrogen receptor-negative invasive breast carcinoma and requires BRCA1. Oncogene. 2009;28(6):843-53.
14. Lu C, Han HD, Mangala LS, Ali-Fehmi R, Newton CS, Ozbun L, et al. Regulation of tumor angiogenesis by EZH2. Cancer Cell. 2010;18(2):185-97.
15. Ferraro A, Mourtzoukou D, Kosmidou V, Avlonitis S, Kontogeorgos G, Zografos G, et al. EZH2 is regulated by ERK/AKT and targets integrin alpha2 gene to control Epithelial-Mesenchymal Transition and anoikis in colon cancer cells. Int J Biochem Cell Biol. 2013;45(2):243-54.
16. Livak KJ, Schmittgen TD. Analysis of relative gene expression data using real-time quantitative PCR and the 2(-Delta Delta C(T)) Method. Methods. 2001;25(4):402-8.
17. Xi Y, Xu P. Global colorectal cancer burden in 2020 and projections to 2040. Transl Oncol. 2021;14(10):101174.
18. Qadir MI, Parveen A, Ali M. Cdc42: Role in Cancer Management. Chem Biol Drug Des. 2015;86(4):432-9.
19. Kamai T, Yamanishi T, Shirataki H, Takagi K, Asami H, Ito Y, et al. Overexpression of RhoA, Rac1, and Cdc42 GTPases is associated with progression in testicular cancer. Clin Cancer Res. 2004;10(14):4799-805.
20. Bachmann IM, Halvorsen OJ, Collett K, Stefansson IM, Straume O, Haukaas SA, et al. EZH2 expression is associated with high proliferation rate and aggressive tumor subgroups in cutaneous melanoma and cancers of the endometrium, prostate, and breast. J Clin Oncol. 2006;24(2):268-73.
21. Krill L, Deng W, Eskander R, Mutch D, Zweizig S, Hoang B, Ioffe O, Randall L, Lankes H, Miller DS, Birrer M. Overexpression of enhance of Zeste homolog 2 (EZH2) in endometrial carcinoma: An NRG Oncology/Gynecologic Oncology Group Study. Gynecol Oncol. 2020;156(2):423-9.
22. Valdés-Mora F, Locke WJ, Bandrés E, Gallego-Ortega D, Cejas P, García-Cabezas MA, Colino-Sanguino Y, Feliú J, Del Pulgar TG, Lacal JC. Clinical relevance of the transcriptional signature regulated by CDC42 in colorectal cancer. Oncotarget. 2017;8(16):26755-70.
23. Chen JF, Luo X, Xiang LS, Li HT, Zha L, Li N, He JM, Xie GF, Xie X, Liang HJ. EZH2 promotes colorectal cancer stem-like cell expansion by activating p21cip1-Wnt/β-catenin signaling. Oncotarget. 2016;7(27):41540-58.
24. Chen Z, Yang P, Li W, He F, Wei J, Zhang T, Zhong J, Chen H, Cao J. Expression of EZH2 is associated with poor outcome in colorectal cancer. Oncol Lett. 2018;15(3):2953-61.
25. Li Y, Sun Z, Liu B, Shan Y, Zhao L, Jia L. Tumor-suppressive miR-26a and miR-26b inhibit cell aggressiveness by regulating FUT4 in colorectal cancer. Cell Death Dis. 2017;8(6):e2892.
26. Si Z, Yu L, Jing H, Wu L, Wang X. Oncogenic lncRNA ZNF561-AS1 is essential for colorectal cancer proliferation and survival through regulation of miR-26a-3p/miR-128-5p-SRSF6 axis. J Exp Clin Cancer Res. 2021;40(1):78.
27. Fussbroich B, Wagener N, Macher-Goeppinger S, Benner A, Fälth M, Sültmann H, Holzer A, Hoppe-Seyler K, Hoppe-Seyler F. EZH2 depletion blocks the proliferation of colon cancer cells. PLoS One. 2011;6(7):e21651.

28. Ohuchi M, Sakamoto Y, Tokunaga R, Kiyozumi Y, Nakamura K, Izumi D, Kosumi K, Harada K, Kurashige J, Iwatsuki M, Baba Y, Miyamoto Y, Yoshida N, Shono T, Naoe H, Sasaki Y, Baba H. Increased EZH2 expression during the adenoma-carcinoma sequence in colorectal cancer. Oncol Lett. 2018;16(4):5275-81.
29. Kodach LL, Jacobs RJ, Heijmans J, van Noesel CJ, Langers AM, Verspaget HW, Hommes DW, Offerhaus GJ, van den Brink GR, Hardwick JC. The role of EZH2 and DNA methylation in the silencing of the tumour suppressor RUNX3 in colorectal cancer. Carcinogenesis. 2010;31(9):1567-75.
30. Gao S, Xue J, Wu X, Zhong T, Zhang Y, Li S. The relation of blood cell division control protein 42 level with disease risk, comorbidity, tumor features/markers, and prognosis in colorectal cancer patients. J Clin Lab Anal. 2022;36(7):e24572.

J Surg Med. 2025;9(7):109-112.
https://doi.org/10.28982/josam.8059

JOSAM

Journal of Surgery and Medicine

e-ISSN: 2602-2079

Case report
https://jsurgmed.com/

A rare cause of childhood chylothorax: Gorham-Stout disease

Yasemin Mocan Çağlar [1], Sinem Can Oksay [1], Ayşe Nur Toksöz Yıldırım [2], Sabriye Gülçin Bozbeyoğlu [3], Saniye Girit [1]

[1] Istanbul Medeniyet University, Department of Pediatric Pulmonology, Istanbul, Turkey
[2] Istanbul Medeniyet University, Department of Pathology, Istanbul, Turkey
[3] Istanbul Medeniyet University, Department of Radiology, Istanbul, Turkey

ORCID of the author(s)

YMÇ: https://orcid.org/0000-0002-9609-478X
SCO: https://orcid.org/0000-0001-9801-3181
ANTY: https://orcid.org/0000-0003-1708-0003
SGB: https://orcid.org/0000-0003-1593-4351
SG: https://orcid.org/0000-0001-7556-6568

Corresponding Author
Saniye Girit
Istanbul Medeniyet University, Faculty of Medicine, Department of Pediatrics, Division of Pulmonology, Göztepe Training and Research Hospital, Istanbul, Turkey
E-mail: saniyegirit@gmail.com

Informed Consent
The authors stated that the written consent was obtained from the parents of the patient presented with images in the study.

Conflict of Interest
No conflict of interest was declared by the authors.

Financial Disclosure
The authors declared that this study has received no financial support.

Published
2025 July 13

Abstract

Gorham syndrome is an extremely rare bone disease, with only a limited number of cases reported worldwide. It is characterized by progressive bone resorption associated with abnormal proliferation of lymphatic vessels, making it a rare case in medical literature. This disorder can lead to serious complications including chylothorax, especially in children. Early diagnosis and treatment are crucial in the prevention of life-threatening outcomes. This report presents a case of a young child with recurrent pleural effusion and bone lesions, eventually diagnosed with Gorham's disease. A three-year-old patient was admitted with recurrent pleural effusion, chylothorax, and pneumothorax. Imaging revealed multiple lytic bone lesions, suggestive of bone destruction. A lung biopsy confirmed lymphatic dilation, supporting a diagnosis of Gorham's disease. The patient's condition was evaluated through a multidisciplinary approach involving pulmonology, pathology, and radiology teams. Treatment included a combination of pharmacotherapy and dietary modifications, which successfully stabilized the patient's condition. The child has since been closely monitored, with no significant recurrence of symptoms. The progression of the disease can be life-threatening, particularly when the thoracic duct is involved, leading to recurrent pleural effusions. In this particular case, early diagnosis through a collaborative medical approach allowed for prompt treatment. Ongoing monitoring is essential in preventing relapses and ensuring long-term health outcomes for the patient.

Keywords: Gorham-Stout disease, chylothorax, pleural effusion, sirolimus

Introduction

Gorham-Stout disease (GSD) is an extremely rare bone disease, with only a limited number of cases reported worldwide. The incidence in children in the UK was 0.0014% (1.4 per 100,000) [1]. The majority of cases are observed in children and young adults without a familial inheritance pattern. The disease is characterized by progressive bone resorption associated with abnormal proliferation of lymphatic vessels. Clinical manifestations vary depending on the location of the affected area and the extent of bone destruction. Involvement of bones forming the chest cage, such as thoracic vertebrae and ribs, lead to prominence of respiratory symptoms [2,3]. We aimed to present a case of a three-year-old patient presenting with chylothorax in the context of the literature.

How to cite: Mocan Çağlar Y, Oksay SC, Toksöz Yıldırım AN, Bozbeyoğlu SG, Girit S. A rare cause of childhood chylothorax: Gorham-Stout disease. J Surg Med. 2025;9(7):109-112.

Case presentation

A three-year-old Caucasian boy presented with a two-week history of fever and cough. He was born at term, weighing 2790 g, via cesarean section. No history of neonatal intensive care unit admission was reported. Vaccinations were up to date for his age. There was no consanguinity between the parents. There was no family history of chronic lung disease, asthma, or tuberculosis.

Past medical history: One year ago, the child presented to a hospital with sudden onset fever, tachypnea, and dyspnea. Bilateral pneumothorax was detected and managed with chest tube insertion, but lung expansion could not be achieved due to massive air leak and 70% saturation. Upon worsening of his clinical condition, a bullous area was excised from the right apex of the lung. Four months ago, he had a fracture of the right femur without a history of trauma. Two weeks ago, a chest tube was inserted due to bilateral pleural effusion detected on a chest X-ray. He was observed with a chest tube for five days, and then referred to our center due to recurrent pleural effusion after tube removal.

Physical examination: Dyspnea, tachypnea, and retractions were observed. His vital signs were saturation: 99%; respiratory rate: 98/min; blood pressure: 96/67 mmHg. Height: 92 cm (-1.52 SDS); body weight: 12 kg (-2.15 SDS). On auscultation, breath sounds decreased on the right side, and crepitant rales were present on the left side. There was no wheezing or rhonchi, nor was there any clubbing or chest deformity. There was a BCG scar. Hepatosplenomegaly was absent. Other system examinations were unremarkable. Laboratory examination revealed: Hb:10.9 g/dl, WBC:5300/mm^3, plt:411000/mm^3, lymphocytes:1900/mm^3. CRP was negative. The chest X-ray showed a cavitary area in the right apex, basal pleural effusion in the right lower lobe, and increased nonhomogeneous infiltration in the bilateral lower lobes (Figure 1). Pleural fluid appeared dirty yellow-white. Triglyceride level was 232 mg/dL; and cholesterol was 67.2 mg/dL, suggestive of chylothorax. Direct radiography showed intramedullary hypodense millimetric lytic lesions at the 4-5th anterior ribs. MRI showed osteolytic signal increase areas in T8-T11-12 vertebral bodies without contrast enhancement (Figure 2) lytic lesions in the left occipital bone (Figure 3). Bone mineral density was -1.87 SDS. Thoracic CT angiography was normal. Whole-body bone scintigraphy revealed abnormally increased metabolism in cervical 6 and thoracic 11-12 vertebral bodies and adjacent ribs. Cystic lesions were seen in the spleen on an ultrasound (Figure 4). Lower extremity radiography revealed callus tissue from the previous fracture in the midshaft of the right femur. Lung tissue excised during bullectomy was reevaluated histopathologically and subpleural lymphatic dilation and cystic lymphatic vessels were observed (Figures 5,6,7).

Based on the multidisciplinary evaluation of the current clinical, radiological, and pathological findings, a diagnosis of GSD was made. For the treatment, oral feeding was maintained, but the diet was modified to include medium-chain triglyceride (MCT)-based foods. The patient received pulse steroid therapy for three days followed by oral prednisolone for 45 days. Due to a lack of response to corticosteroid therapy, alpha interferon 2-beta was initiated, starting at 1.5 million U/m^2 three times a week for two weeks, then increased to 3 million U/m^2. Propranolol was administered at a dose of 4 mg/day for four months. As pleural effusion persisted, both interferon 2-beta and propranolol were stopped and sirolimus treatment was introduced at a dose of 0.8mg/m^2/day twice daily in liquid form for six months. The patient was monitored with sirolimus blood level and no side effects were observed. After six months of sirolimus therapy, the patient's symptoms fully resolved. During the five-year follow-up period, no new bone fractures or pleural effusion occurred, and the patient has continued on the MCT diet.

Figure 1: X-ray: Intramedullary hypodense millimetric lytic lesions in the anterior vertebral bodies of 4-5 (white arrows), fusion defect in the vertebral bodies of 5-6, linear band-like pleuroparenchymal in the lower lobe of the right lung, basal pleural effusion with a diameter of 7 mm

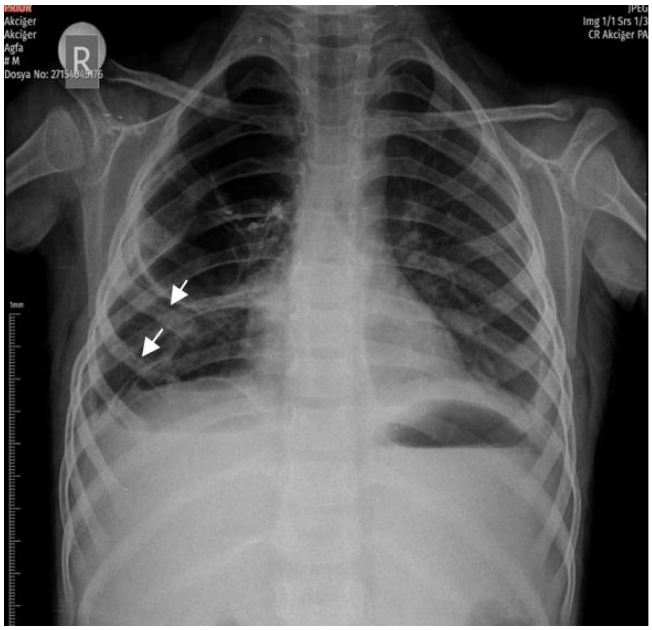

Figure 2: MR: Signal increases without contrast uptake are present in the vertebral bodies of T8-T11-12 (white stars).

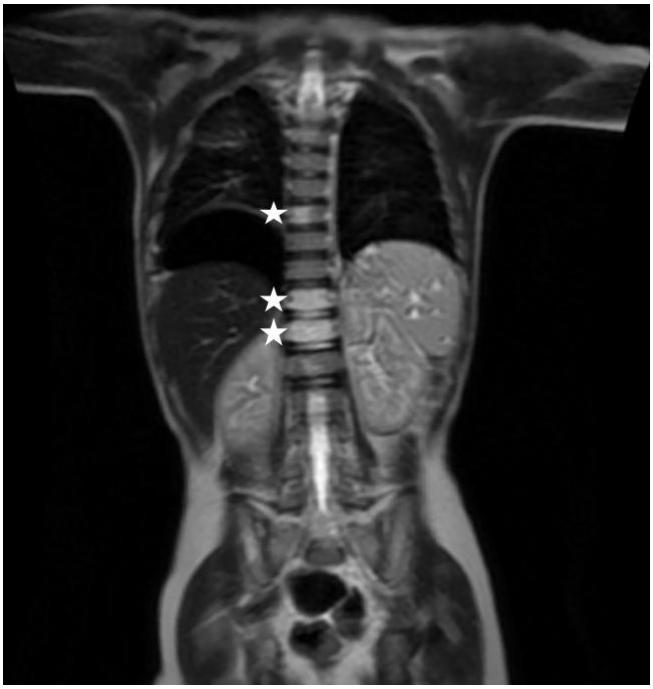

Figure 3: Lytic lesions at the occipital bone (black stars). Figure 1d: US: Cystic lesions in the spleen (thick black arrows).

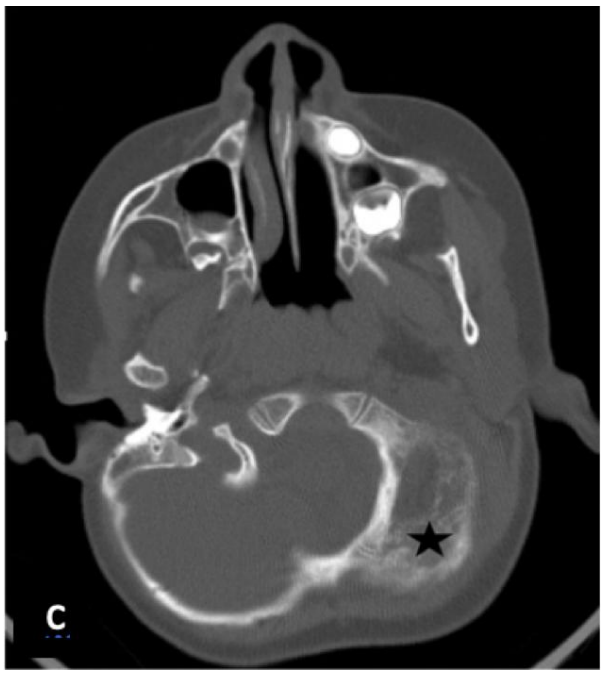

Figure 4: US: Cystic lesions in the spleen (thick black arrows).

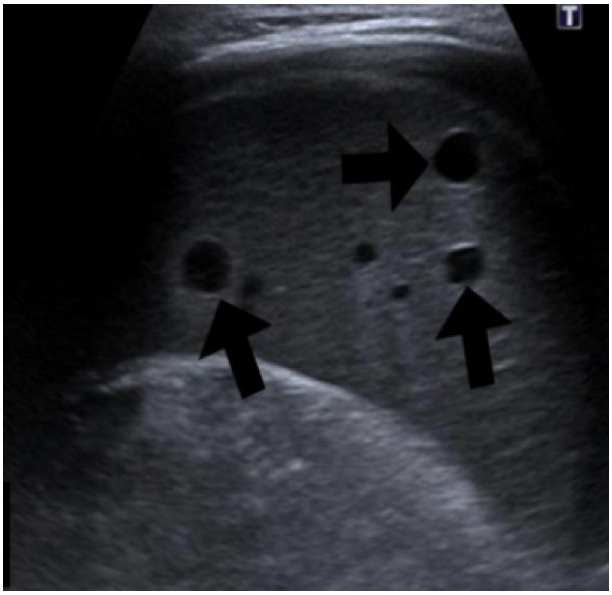

Figure 5: Subpleural lymphatic dilatations (thick blue arrow). Stained with hematoxylin and eosin, and magnified 40 times.

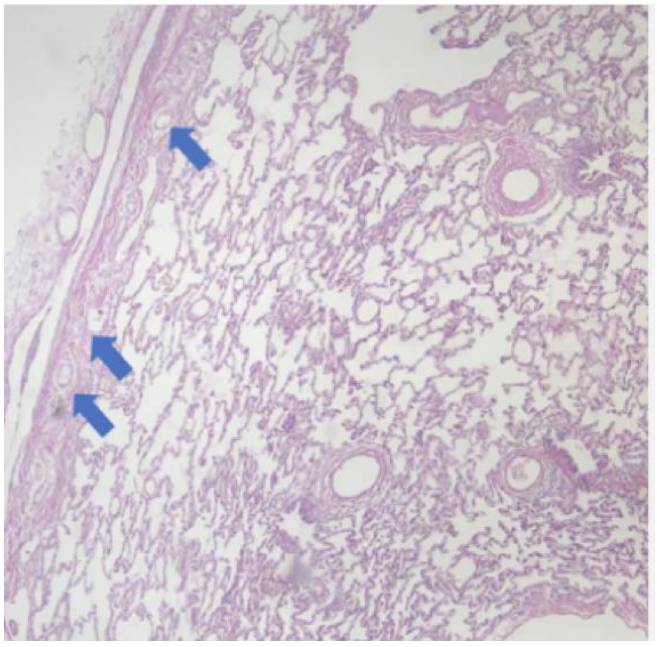

Figure 6: Subpleural cystic lymphatic dilatations (blue arrow), bull formation (blue star), emphysematous areas (green star). Stained with hematoxylin and eosin, and magnified 40 times.

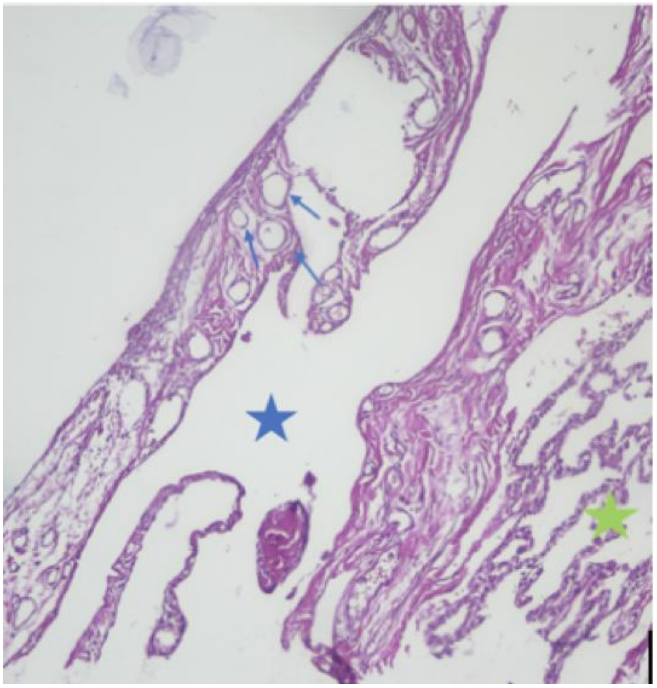

Figure 7: Enlarged lymphatic vessels (pink arrow) (Immunohistochemical d240 analysis X40)

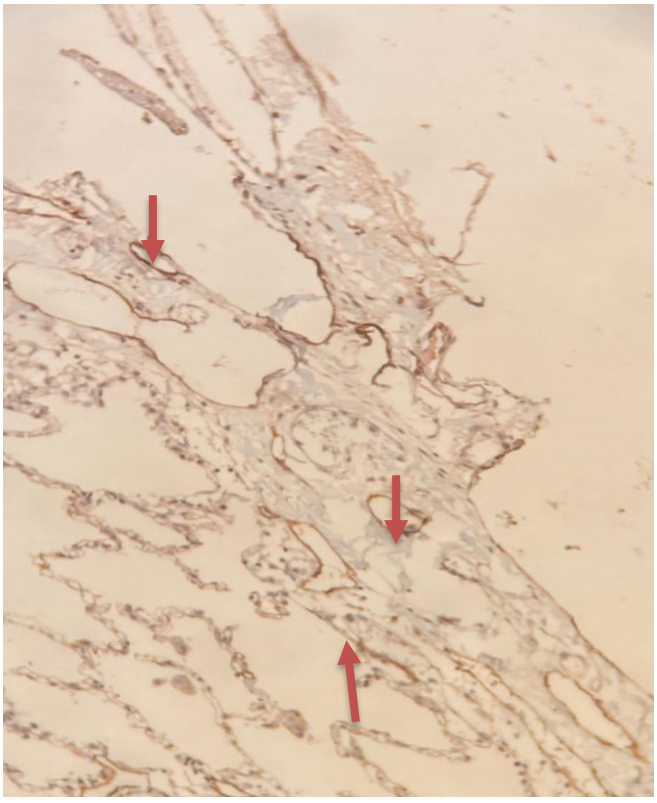

Discussion

Gorham-Stout disease can progress aggressively or proceed with spontaneous remission, characterized by vascular and lymphatic channel proliferation and bone osteolysis. The disease may not be detected until it presents with clinical symptoms, such as pathological bone fracture, pericardial effusion, or chylothorax [2,3].

The etiology of chylothorax includes various factors, such as lymphatic malformations, injury to the thoracic duct, and lymphadenopathy, as well as mass effect, surgery, and trauma. In the presence of benign chylous effusion and lytic bone lesions with an unidentified etiology, GSD, a subgroup of complicated

lymphatic anomalies, should be considered in the differential diagnosis [4]. The incidence of chylothorax in patients with GSD has been reported to be 22-44% in previous years. However, in a 2022 study evaluating the etiology of chylothorax in childhood, GSD accounted for 30% of the causes of chylothorax. In the same study, bone involvement was detected, especially vertebrae, in all seven cases with GSD [5]. Extraosseous involvement in GSD is also known as splenic involvement [6]. Our specific case demonstrated cystic lesions indicative of splenic involvement of the disease.

The symptoms of our patient began at the age of two, which is quite an early onset, since GSD is often seen in older children and adolescents [3,5]. The absence of any symptoms during the prenatal and postnatal periods rules out reasons such as hydrops fetalis or injury to the thoracic duct at birth. There was no history of surgery or injury in the period leading up to the development of pleural effusion in our patient. Although chylothorax can occur secondary to high central venous pressure, various tumoral causes, and infections and sarcoidosis causing pressure, these were excluded in our case.

The diagnosis of Gorham-Stout disease in this patient took six months due to its rarity and the absence of standard treatment guidelines. The multidisciplinary approach, involving pulmonology, pathology, oncology, and radiology teams, was crucial in reaching the correct diagnosis and selecting an appropriate treatment strategy amidst the challenges posed by this complex condition.

The prognosis of GSD varies depending on the extent of involvement. While spontaneous remission is possible, the disease can also progress aggressively and lead to life-threatening complications. Treatments like sirolimus offer hope, but careful monitoring is necessary due to potential side effects and the risk of recurrence. With early diagnosis and treatment, long-term survival is achievable, though complications such as pleural effusion may recur even years later. Although there is no standard care protocol for chylothorax treatment, the most recommended approach is to start with dietary changes (TPN, MCT), followed by octreotide and finally surgical intervention [3,5,7]. Surgery is recommended when there is a significant deterioration in nutritional status despite conservative treatment or when daily chylous fluid drainage exceeds 10 ml/kg.

However, because conservative treatments may take time to be effective, alternative treatments have been proposed. Such alternatives include propranolol, a β2 adrenergic receptor blocker that reduces proangiogenic factor expression, and alpha-interferon, which inhibits lymphatic vessel proliferation [3]. Sirolimus, an mTOR inhibitor, has shown efficacy in treating lymphatic malformations, including Gorham-Stout disease. However, its use is associated with several potential side effects. Common adverse effects observed in children include stomatitis, gastrointestinal issues, hyperlipidemia, and infections due to its immunosuppressive properties. In rare cases, sirolimus can cause thrombocytopenia and impair wound healing. Despite these risks, the benefits of sirolimus in managing lymphatic malformations often outweigh the side effects when monitored closely in a controlled setting [8].

Conclusion

Gorham-Stout disease should be considered in chylothorax with accompanying bone lesions in patients of all ages. Treatment strategies for GSD are generally experimental due to the lack of randomized controlled trials and standardized guidelines. Treatment is aimed at alleviating symptoms, preventing disease progression, and preserving skeletal integrity. Surgical interventions and angiogenesis inhibitors such as sirolimus may be tried in selected patients.

References

1. Haines C, Walsh B, Fletcher M, Davis PJ. Chylothorax development in infants and children in the UK. Arch Dis Child. 2014;99(8):724–30.
2. Dellinger MT, Garg N, Olsen BR. Viewpoints on vessels and vanishing bones in Gorham-Stout disease. Vol. 63, Bone. Elsevier Inc.; 2014. p. 47–52.
3. Ozeki M, Fujino A, Matsuoka K, Nosaka S, Kuroda T, Fukao T. Clinical Features and Prognosis of Generalized Lymphatic Anomaly, Kaposiform Lymphangiomatosis, and Gorham-Stout Disease. Pediatr Blood Cancer. 2016 May 1;63(5):832–8.
4. Riley LE, Ataya A. Clinical approach and review of causes of a chylothorax. Vol. 157, Respiratory Medicine. W.B. Saunders Ltd; 2019. p. 7–13.
5. Büyükşahin HN, Emiralioğlu N, Özcan HN, Sunman B, Güzelkaş İ, Alboğa D, et al. Evaluation of Clinical Findings in Children with Chylothorax: A Descriptive Study. Turkish Archives of Pediatrics. 2023 Jan 1;58(1):28–33.
6. Kotecha R, Mascarenhas L, Jackson HA, Venkatramani R. Radiological features of Gorham's disease. Clin Radiol. 2012;67(8):782–8.
7. Ozeki M, Fukao T. Generalized Lymphatic Anomaly and Gorham-Stout Disease: Overview and Recent Insights. Vol. 8, Advances in Wound Care. Mary Ann Liebert Inc.; 2019. p. 230–45.
8. Wiegand S, Dietz A, Wichmann G. Efficacy of sirolimus in children with lymphatic malformations of the head and neck. Vol. 279, European Archives of Oto-Rhino-Laryngology. Springer Science and Business Media Deutschland GmbH; 2022. p. 3801–10.